Assessment of Oil Recovery Methods for Reservoirs in the Flemish Pass Basin

by Chad LaFitte

A Thesis submitted
to the School of Graduate Studies in partial fulfillment of the
requirements for the degree of

Master of Engineering (M.Eng.)

Faculty of Engineering and Applied Science
Memorial University of Newfoundland

February 2021

St. John’s, Newfoundland and Labrador

Acknowledgements

This research was conducted under the guidance of, and with continued support from the following people and groups:

- Memorial University of Newfoundland
    - Dr. Lesley James, Academic Supervisor, Petroleum Engineering
- Husky Energy, Atlantic Region Developments team; specifically,
    - James Carter, P.Geol.
      Geo-modeler for full-field static development model(s)
    - Stephen Kearsey, P.Geoph.
      Structural modeler for full-field static development model(s)
- Equinor Canada, Reservoir and Production Technology (PETEC) team

Abstract

In recent years, the Flemish Pass Basin has been gaining momentum as an area of potential high-volume resources on the frontier of remote, deep-water offshore oil exploration. This simulation study utilizes three sector models representing regional, discovered reservoirs, and two tuned fluid models representing oil sampled from wells in the Flemish Pass Basin.

This study evaluates three secondary oil recovery methods, water flooding, gas flooding, and water-alternating-gas (WAG) flooding. These methods are simulated using ECLIPSE reservoir simulator [1] within the sector models from three different quality reservoirs, and the two different quality fluid models. This is accomplished through a sensitivity analysis of the representative Flemish Pass fluid and reservoir models, using both five and twenty year forecast simulation cases.

The evaluation results capture an inherent uncertainty given the varied reservoir and fluid qualities while the depletion plan is controlled by recovery method. Dynamic modelling results in a range of possible recovery factors from eighteen simulation cases which quantifies the relative benefit of each oil recovery method.

Comprehensive results indicate that implementing WAG as a secondary recovery method can yield a 4% to 10% increase in recovery factor over water flood or gas flood. WAG is usually considered a late-life enhanced oil recovery (EOR) method or tertiary recovery method. Using WAG for secondary recovery is much less common.

Implementing WAG in the light oil reservoir yields a ~10% increase in recovery factor over both water flood and gas flood. Using WAG in the medium oil cases yields a 4% to 9% increase in recovery factor over water flood, and a 2% to 16% increase in recovery factor over gas flood. The most benefit from WAG is observed in the ultra-high-quality reservoir. The medium oil responds best to the gas injection phase of the WAG cycle so it may be useful to optimize the cycle such that gas is injected for a longer duration relative to the water injection cycle. Additionally, secondary WAG may extend the production plateau up to 80% depending on the reservoir quality, fluid characteristics, and production constraints.

In terms of using WAG as a tertiary recovery method, tertiary WAG is observed to be most beneficial in low to medium quality reservoirs. Tertiary WAG extends the duration of production and results in a consistent ~4% increase in recovery factor over water flooding.

Study results go on to quantify the differences in water and gas breakthrough as a factor of pore volume injected (PVI). The conclusions will further provide indication of which reservoirs are best suited for each recovery method.

Table of Contents

Acknowledgements ... ii
Abstract ... iii
List of Tables ... v
List of Figures ... v
List of Abbreviations ... vi
1. Introduction ... 8
2. Literature Review ... 11
2.1. Introduction ... 11
2.2. Scope ... 11
2.3. Identification and Filtering ... 13
2.4. Discussion of Relevant Literature ... 14
2.5. Summarized Literature Findings ... 21
3. Methodology ... 22
3.1. Geological Sector Models ... 22
3.2. Fluid Data and Characteristics ... 25
3.3. Fluid Modelling ... 26
3.4. Additional Dynamic Model Inputs ... 33
4. Results and Discussion ... 41
4.1. Overview ... 41
4.2. Ultra-High-Quality (UHQ) Reservoir Results ... 51
4.3. High-Quality (HQ) Reservoir Results ... 54
4.4. Low-Quality (LQ) Reservoir Results ... 56
4.5. WAG Secondary vs. Tertiary (EOR) Recovery Methods ... 58
5. Conclusions and Recommendations ... 61
5.1. Conclusions ... 61
5.2. Recommendations ... 63
6. References ... 64
Appendix A: UHQ Test Results with WAG Hysteresis ... 67

List of Tables

Table 1: Mean Sector Model Parameters 23
Table 2: Tabulated Overview of Light Oil Sample Properties 26
Table 3: Tabulated Overview of Medium Oil Sample Properties 26
Table 4: Selected Light Oil Experiments for Plus Regression 27
Table 5: Tabulated Recovery Factor differences for all Scenarios 42
Table 6: Tabulated Recovery Factor by PVI Increments (UHQ, Light Oil) 52
Table 7: Tabulated Recovery Factor by PVI Increments (UHQ, Medium Oil) 52
Table 8: Tabulated Recovery Factor by PVI Increments (HQ, Light Oil) 55
Table 9: Tabulated Recovery Factor by PVI Increments (HQ, Medium Oil) 55

List of Figures

Figure 1: Bay du Nord (BdN) Project Location [10] 10
Figure 2: Modified schematic of a secondary recovery method [30]. 12
Figure 3: Literature Review Document Identification and Filtering Process 13
Figure 4: Pie Charts by Christensen et al. showing WAG Field Applications [14] 15
Figure 5: Ultra-High-Quality Sector Model, K-Slice 24
Figure 6: High-Quality Sector Model, K-Slice 24
Figure 7: Low-Quality Sector Model, K-Slice 24
Figure 8: Composition Chart for Light and Medium Oil Samples 25
Figure 9: Light Oil Lumping Scheme 26
Figure 10: Light Oil, PVT EoS Tuning with Plus Regression 28
Figure 11: Light Oil, PVT EoS Tuning with Characterized Regression 30
Figure 12: Medium Oil Lumping Scheme 31
Figure 13: Medium Oil, PVT EoS Tuning with Characterized Regression 32
Figure 14: Water Saturation (J-Function) Models 36
Figure 15: Generic water-oil curves influenced by LET parameters (Equinor ASA, 2017) 37
Figure 16: UHQ-HQ Reservoir, Oil-Water Drainage Relative Permeability Curves 38
Figure 17: LQ Reservoir, Oil-Water Drainage Relative Permeability Curves 38
Figure 18: UHQ-HQ Reservoir, Oil-Gas Drainage Relative Permeability Curves 38
Figure 19: LQ Reservoir, Oil-Gas Drainage Relative Permeability Curves 38
Figure 20: Simulation Case Structure 40
Figure 21: Results, Recovery Factor (%) by Simulation Case 41
Figure 22: Recovery Factor charts for Light Oil cases 43
Figure 23: Recovery Factor charts for Medium Oil cases 45
Figure 24: Extended Case 'Water flood' Results 46
Figure 25: Extended Case 'Gas flood' Results 48
Figure 26: Extended Case ‘WAG flood’ Results 49

Figure 27: Results for UHQ, Light and Medium Oil cases 51
Figure 28: Results for HQ, Light and Medium Oil cases..... 54
Figure 29: Results for LQ, Light and Medium Oil cases 56
Figure 30: UHQ Reservoir, WAG, Secondary vs. EOR Recovery Method 58
Figure 31: HQ Reservoir, WAG, Secondary vs. EOR Recovery Method..... 59
Figure 32: LQ Reservoir, WAG, Secondary vs. EOR Recovery Method 60
Figure 33: Simulation Results comparing UHQ Light Oil cases with and without WAG Hysteresis 68

List of Abbreviations

Abbreviation	Definition
ACTNUM	Active grid block identification for blocks in a reservoir model
API	American Petroleum Institute gravity
BSW	Basic Sediment and Water
C-NLOPB	Canada-Newfoundland and Labrador Offshore Petroleum Board
CO_2	Chemical formula for Carbon Dioxide
DST	Drill Stem Test
EOR	Enhanced Oil Recovery
ES	Evolutionary Strategy
FVF	Formation Volume Factor
GINJ	Gas Injection
GMDH	Group method of data handling
GOR	Gas-Oil Ratio
HAFWL	Height above free water level
HQ	High-Quality
J	J-Function, Leverett
K	Permeability
LBC	Lohrenz-Bray-Clark
LET	Relative permeability correlation where L (lower), E (elevation), and T (top) are empirical parameters
LQ	Low-Quality
MAX	Maximum
MDT	Modular Dynamics Testing
MIN	Minimum
MMP	Minimum Miscibility Pressure
NL	Newfoundland & Labrador
NPV	Net Present Value
OBM	Oil Based Mud
OOIP	Original Oil In Place

P_c	Capillary Pressure
PETEC	Petroleum Technology
PROPS	A simulation input file that details fluid and rock properties
PSO	Particle Swarm Optimization
PVI	Pore Volume(s) Injected, ratio
PVT	Pressure, Volume, Temperature
RCA	Routine Core Analysis
RF	Recovery Factor
SCAL	Special Core Analysis
SDL	Significant Discovery License
SPE	Society of Petroleum Engineers
SSE	Sum of Squares Error
S_w	Water Saturation
S_{wco}	Connate Water Saturation
UHQ	Ultra-High-Quality
WAG	Water-Alternating-Gas
WCUT	Water Cut
WINJ	Water Injection
θ	Contact Angle
ρ	Density
∅	Porosity
σ	Surface Tension

1. Introduction

This research focuses on evaluating three types of oil recovery methods in three different quality sector models that represent discovered, clastic, sandstone reservoirs in the Flemish Pass Basin.

This study will also evaluate different quality oils via two distinct fluid models that are based on sampled fluids from exploration wells in the basin. The goal of the study framework is to capture a broad degree of uncertainty by incorporating various quality oils and reservoirs while varying the secondary oil recovery method.

There are several stages to oil recovery [2]. Primary recovery generally utilizes a single producer well and relies on rock and liquid expansion, water drive, gas cap drive, or a combination of these natural drive mechanisms [2]. Secondary recovery usually refers to either water flood or immiscible gas flood [2], both of which require two wells, a producer and an injector, to effectively sweep the hydrocarbons toward the producer location [2]. Both of these secondary recovery methods will be used in this study; however, the gas flooding will occur at miscible conditions, above the minimum miscibility pressure (MMP). This will be controlled in the model by setting a minimum flowing bottom hole pressure constraint on the production well that is high enough to ensure every grid cell in the sector model maintain a pressure above the MMP. In terms of tertiary recovery, there are many options available to fully exploit a reservoir [3]. Water-alternating-gas (WAG) flooding is a common tertiary and enhanced oil recovery (EOR) method that has historically been most used in late-life of field situations [3]. Instead of waiting until late-life to implement water-alternating-gas injection as an EOR method, this study implements WAG as a secondary recovery method at first oil.

Water-alternating-gas injection combines improved sweep by the water phase in low permeability intervals with improved sweep by the gas phase in high permeability intervals [4]. These benefits mean that using water-alternating-gas injection can improve overall sweep efficiency relative to using only one of the two injection phases. As a result of this improved sweep, hydrocarbon recovery also improves which positively effects the Net Present Value (NPV) of the well pair and the associated development project.

WAG generally extends the life of a field given that the improved sweep efficiency extends the production period where the oil production rate is greater than the minimum economic oil production rate. This extended field life spreads the cost of the asset across additional years which reduces the annual depreciation of capital expenditure [5].

In addition to direct economic benefits, WAG often uses the field produced gas for reinjection during the gas phase injection cycle. Being able to cycle produced gas back through the reservoir means that the produced gas no longer requires subsurface disposal or flaring. This is a significant benefit for the facility's gas handling system and associated production constraints, as well as the environment, and project economics.

Alternative options include having to flare the gas, subject to regulatory constraints and environmental considerations, or having to dispose of the gas to the subsurface. Subsurface gas disposal equates to large capital costs for drilling, completing, and tying in a gas disposal well. Using produced gas for reinjection avoids these alternative options and their potential negative effects.

It is also important to understand some associated challenges with utilizing WAG; such as, higher cost of wellhead infrastructure compared to single phase water or gas injection, and increased gas cycling through the reservoir and production systems, which can take a toll on facilities equipment. Wear on equipment is largely dependent on the gas composition, production and injection rates, and the equipment materials. Fortunately, these parameters can be largely considered during the design phase and accounted for.

The Flemish Pass Basin is located roughly 480 km East-Northeast of St. John's, NL, Canada, in the remote, deep water of the North Atlantic ocean. The average water depth is 1,100m and the basin is bounded by the Grand Banks to the West and the Flemish Cap to the east [6].

The Flemish Pass has been undergoing evaluation since the early 1980's, with the first exploration well, Baccalieu I-78, a dry hole, drilled in 1985 [7]. Drilling picked back up in the mid-2000's with the well Mizzen L-11 (oil show), Mizzen O-16, the first oil discovery well in the basin, and Mizzen F-09 (wet) in 2011 [7]. From 2013 to 2017 an additional fifteen exploration and appraisal wells, including sidetracks, were drilled in the basin, leading to 'Significant Discovery Licenses' (SDL's) being awarded for Mizzen, Bay du Nord, Baccalieu, and Harpoon discoveries [8].

Given the increased activity in the past two decades, the Flemish Pass is evolving into a potential hub for large-scale development; however, at the time of writing, development plans have yet to be submitted for any specific fields [9].

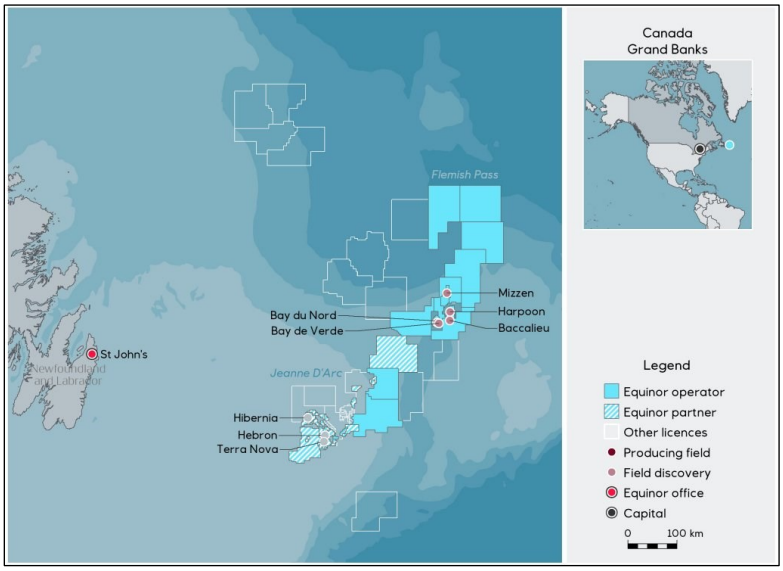

Figure 1: Bay du Nord (BdN) Project Location [10]

The results of this study will quantify the benefits for each of the recovery methods based on recovery factor, for each of the fluid and sector models that represent discoveries throughout the Flemish Pass Basin. The simulations provide unique insight into how each reservoir responds to the various recovery methods depending on flow characteristics and phase behaviour. Conclusions focus on extending the duration of production plateau, delaying gas or water breakthrough, quantifying the pore volumes injected when breakthrough occurs, and understanding the changes in recovery factor between recovery methods, reservoirs, and fluid models.

The workflow involves simulating production from a single well-pair in three sector models that have been extracted from larger, full-field development scenarios. These three sector models have been cropped so that they represent roughly 1.0 x 1.0 kilometre regions. The sector models are designated as Ultra-High-Quality (UHQ), High-Quality (HQ), and Low-Quality (LQ), with mean sandstone permeability and porosity of 3.8 Darcy, 25 % (UHQ), 1.6 Darcy, 22 % (HQ), and 166 millidarcy, 20 % (LQ). The fluid models are based on multiple oil samples of light, sweet crude, around 36 °API, and medium, sweet crude, around 21 °API. Both fluid models are tuned to appropriate Equations of State for compositional modelling. The Peng Robinson Equation of State (EoS) model is used for the light oil, and the Peng Robinson predictive 1978 EoS is used for the medium oil. Both fluid models make use of the Temperature dependent Peneloux density correction and a Lohrenz-Bray-Clark (LBC) viscosity model.

All simulations are performed using Schlumberger Eclipse 300 [1] for compositional dynamic modelling. Compositional modelling provides a “multicomponent reservoir fluid description for compositional changes” [1]. This method performs equation of state calculations to precisely model phase behaviour. The alternative, black oil simulation,

uses a much simpler approach of tabulated variables and pressures to look up and interpolate fluid parameters.

2. Literature Review

2.1. Introduction

This study examines the benefits of three oil recovery methods for depleting different quality reservoirs containing light and medium API oils. The three recovery methods being evaluated are water flooding, gas flooding, and water-alternating-gas (WAG) flooding. WAG is generally used as an enhanced oil recovery (EOR) method. When used for EOR purposes, WAG is applied to a depletion scheme after years of secondary recovery from waterflooding or gas flooding; however, this study will examine implementing a WAG scheme immediately at first oil, as a secondary recovery method.

Throughout the literature review sourcing process it became clear that many papers related to WAG serve as case studies of particular offshore fields [11] or very specific simulation studies aimed at evaluating WAG recovery as an EOR technique [12]. The novelty of this study comes from its evaluation of WAG as a secondary recovery method, compared against water flooding and gas flooding in a sensitivity analysis format. In addition, this simulation study maintains regional significance by focusing on reservoirs and fluids that have been discovered in the Flemish Pass Basin. Utilizing data from these discoveries allows for the evaluation of regional uncertainty through a simulation-based sensitivity study.

This study follows a systematic approach, using a sensitivity analysis to evaluate the benefits of each recovery method and determine which is most beneficial in the various geological and fluid environments. The reservoir models maintain a regional focus on subsurface parameters that have already been encountered in wells in the Flemish Pass Basin. This regional focus on the Flemish Pass Basin is another example of novelty, accomplished by extracting sector models from full-field static models that have been created for various potential Flemish Pass developments.

The ultimate goal is to quantify and compare the observed benefits of each recovery method in the initial five-year period of oil production. This is generally considered the time-frame that is most commercially impactful to a large-scale offshore development project.

2.2. Scope

This literature review is defined and constrained by the following categories. Each constraint is based on the goal of identifying materials that are focused on offshore oil developments worldwide. Specific consideration is given to the geological, fluid quality, and phase behaviour conditions analogous to those observed in wells drilled in the Flemish Pass Basin.

2.2.1. Sources

Sources are constrained to Google Scholar, OnePetro, and the Petroleum Abstracts TULSA® Database.

2.2.2. Focus Area

Geographic focus area is worldwide. Offshore oil wells and fields. Exclude onshore.

Exploration, development, producing, or abandoned stage of field life.

2.2.3. Reservoir Geology

Conventional reservoir with clastic sedimentary rock, consolidated to near-unconsolidated.

Very-fine grain to coarse grain sandstone as the primary reservoir rock.

Include horizontal permeability >25mD, effective porosity >15%.

Exclude carbonate reservoirs.

2.2.4. Hydrocarbon Phase

Focusing on black oil reservoirs. Reservoir Temperature < Critical Temperature. Undersaturated and saturated conditions.

Exclude gas condensate and volatile oil reservoirs.

2.2.5. Hydrocarbon Density

Include only medium and light crude oils (21.0 ≤ °API ≤ 42.0).

2.2.6. Recovery Methods

Water flooding, Gas flooding, WAG flooding.

Focus on gas flood and WAG flood using produced solution gas, and under miscible flood conditions; however, documentation related to immiscible floods and other variations of injection gas; such as, CO2, will also be documented.

Exclude chemical injection, steam injection, carbonated water injection, unconventional recovery methods (near-wellbore stimulation), and other EOR techniques.

Exclude considering the effects of brine salinity, e.g. altered water composition WAG.

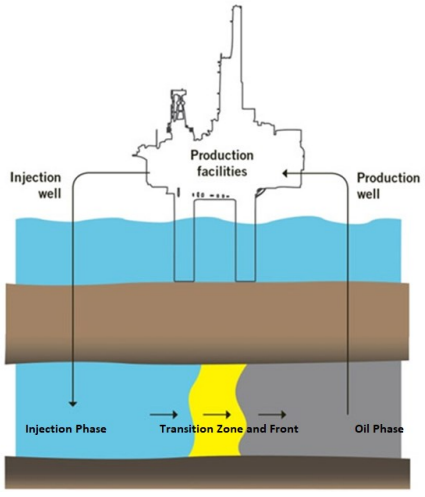

Figure 2: Modified schematic of a secondary recovery method [30].

2.3. Identification and Filtering

Based on the discussed parameters, a search is conducted using the three noted sources. Twenty-one documents are identified as relevant based upon titles and abstracts alone. All twenty-one of these candidate documents are downloaded and further reviewed for applicability as outlined by the Scope.

As a result of this review, a final grouping of seven documents are flagged as 'final' references that have direct applicability to the study subject. The identification and filtering process is mapped in Figure 3 below.

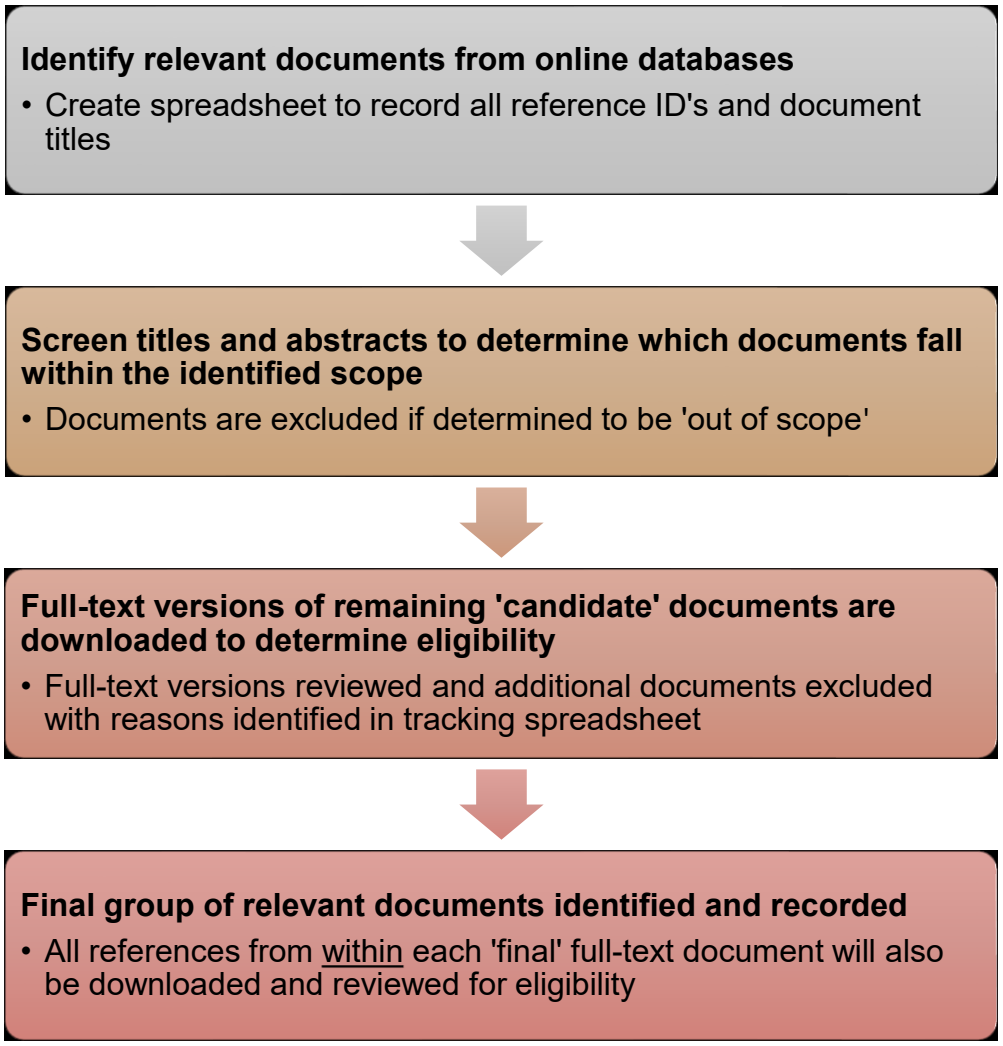

Figure 3: Literature Review Document Identification and Filtering Process

2.4. Discussion of Relevant Literature

A final group of relevant documents has been selected through the identification and filtering process. Several papers were reviewed in detail and their findings categorized based on the following hierarchy.

- Field Experience
    - Regional
    - Global
- WAG Parameters
    - Field scale
    - Core scale
    - Machine learning
- Effects of Hysteresis

A summary of the literature findings can be found in the next section. The summary focuses on the overall results and theoretical indications that have been extracted from all of the relevant documentation.

2.4.1. Field Experience

2.4.1.1. Regional

The Terra Nova offshore oil field, located in the Jeanne d'Arc Basin, came online roughly twenty years ago. Haugen et al. published a paper in 2007 covering the lessons learned after the first five years of production with a section focusing on the injection of a rich gas for gas flood, near or above miscible conditions [11].

The Graben region of the Terra Nova field was designated for gas injection, with a total of three gas injector wells planned; however, due to delays in commissioning, the two associated production wells produced on primary for some time until the gas injectors were brought online [11]. The startup of gas injection quickly supported the producers and brought the reservoir pressure back up [11].

The measured producer GOR associated with these gas injectors has been slower to increase than originally planned – originally designed to be three to five-year wells – yet now they should be able to produce for the life of field before gassing out between 3,000 to 7,000 Sm^3/Sm^3 GOR at end of life [11].

Compositional tracking and simulation for the gas flood regions has indicated that miscible flow development may be occurring, but at the time this paper was written, more historical data was needed to confirm [11]. The discussion suggests that injecting more gas to increase reservoir pressure could lead to a fully miscible phase behaviour scenario; however, this would reduce the solution gas availability which could negatively impact other parts of the field [11]. This is where the option of WAG comes in which generally uses less gas than a pure gas flood scenario. Injectors alternate between water and gas

injection. Gas is injected into a single well for a defined WAG cycle duration while water is injected into the other wells for the same cycle [13]. At the end of the cycle, the gas injection shifts to another well. By cycling the gas injection from well to well in a full field development, there is enough produced gas preserved so that gas is available to be used in other areas of the production system. This is common industry practice. Examples of other potential uses for produced gas include downhole gas lift and operational fuel gas requirements where produced gas is used to run topsides equipment; such as, main power generators.

Using the process of alternating water and gas injection between a set of injection wells allows the operator to maintain reservoir pressure above the minimum miscibility pressure (MMP) without infringing on other production system gas requirements.

When the Terra Nova paper by Haugen et al. was published in 2007, the option of implementing WAG was presented in the paper as a 'future challenge' for the Terra Nova field, with implementation under miscible and immiscible scenarios still being considered [11]. Although the conclusions do not directly relate to the performance metrics of gas flood and WAG flood, the holistic view gives insight into the difficult and ongoing production decisions required to optimize a field with all three phases in play [11].

2.4.1.2. Global

In 2001, Christensen et al. published a review of fifty-nine oil fields and their independent experiences with WAG [14]. This review paper is a valuable piece of literature and has been cited by many researchers since it was first published.

From the analysis, around 80% of the studied fields had originally planned for miscible WAG flooding. This statistic further alludes to an operator's preference to maintain reservoir pressure above the minimum miscibility pressure whenever possible. Based on the full-field data, miscible WAG injection resulted in a mean 9.7% increase in recovery factor, versus 6.4% for immiscible WAG [14]. It is also observed that enhancing the injection gas by adding CO_2 was able to further increase recovery factor; however, it should be noted that CO_2 injection has the potential to lead to corrosion problems throughout the production system [14].

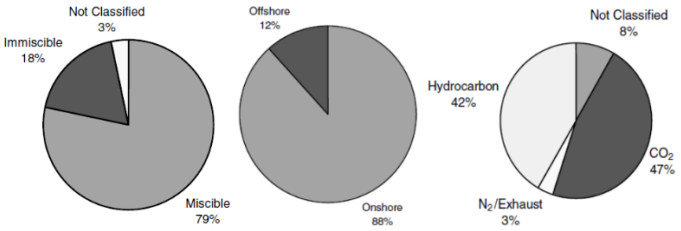

Figure 4: Pie Charts by Christensen et al. showing WAG Field Applications [14]

Only a small percentage of the fifty-nine oil fields attempted WAG injection during the early stages of production where the implementation would be considered secondary recovery. Those that did use WAG for secondary recovery are the more recently developed fields in the North Sea [14]. This reiterates the fact that WAG has only recently been considered viable as a non-EOR technique. Additionally, only six of the fifty-nine fields are located in offshore environments. All six offshore fields used produced hydrocarbons for reinjection gas, with three of the six targeting miscible reservoir conditions [14].

Many offshore fields have excess produced gas that cannot be flared for environmental reasons. In these cases, the excess produced gas is often sold to market. This is common in regions where export gas pipelines exist. Otherwise, excess produced gas must be reinjected into gas storage reservoirs. Implementing water-alternating-gas injection provides a useful alternative for excess gas by reinjecting it in order to directly enhance sweep efficiency, increase recovery, and add value. Christensen et al. conclude by stating that, “The majority of these projects have resulted in a significant incremental oil recovery, generally about 5% to 10%” [14]. These documented results ultimately support WAG as a viable secondary recovery method and a consistent means to improve recovery, with the added benefit of reducing gas flaring and capital spending for drilling disposal wells.

2.4.2. WAG Parameters

2.4.2.1. Field scale analysis

It is common in the development stage of a project to plan for and model fully miscible gas flooding and WAG flooding. In reality, it may prove difficult or impossible to maintain the reservoir pressure above the minimum miscibility pressure for the entire duration of a field’s production. A 1998 paper by Christensen et al. [15] approaches a real-world simulation study by using both compositional and black oil fluid models, and a heterogeneous sandstone reservoir – representing a producing oil field in the North Sea – to compare water flooding to near-miscible WAG flooding. This is a very reasonable perspective as injection conditions often fluctuate between miscible and non-miscible reservoir conditions in real field conditions. Additionally, this study evaluates relative permeability models, with and without hysteresis, in order to evaluate the dynamic fluid effects on recovery [15].

From the simulations, WAG is determined to result in a higher recovery factor than a standard water flood recovery, increasing the sector model recovery factor by approximately 3% [15]. Using continuous gas flood alone results in a recovery factor increase of 1% over water flood [15]. For optimizing the WAG injection parameters, it was determined that using a wet injection gas resulted in an additional 3.4% recovery compared to dry gas injection [15]. Based on the discussed results, using a wet injection gas and maintaining a high gas-to-water injection ratio are both beneficial to recovery [15]. Wet gas is defined as natural gas that typically contains less than 85% methane and an appreciable proportion of hydrocarbon compounds heavier than methane [16].

Ultimately, learnings from the cited works indicate that gas flooding and WAG flooding can often increase the recovery factor over water flooding when the reservoir and fluid characteristics are favorable [15]. This is especially valid where optimization of the WAG scheme is less constrained by the production system and facility bottlenecks such as gas compression limits. The results discussed in Section 4: Results and Discussion will attempt to better quantify the benefits of each recovery method in the specific reservoir and fluid conditions being considered within this sensitivity study.

To achieve a fully optimized injection scheme, it would be ideal to run a dynamic uncertainty analysis using several of the primary input parameters, such as injection ratio and injection cycle durations, in order to gain an understanding of the influence and material impact of each parameter.

A recent paper by Afzali et al. provides an overview on the history, theory, and application of WAG injection [3]. The paper covers a range of documented examples; including, field case studies, laboratory experiments, and simulation studies [3]. These examples are used to summarize many of the applications, operational challenges and remedies, and the effects of subsurface variables on the performance of WAG [3]. The contents of this paper are segregated by topic and discussed in more detail below.

The first topic, reservoir heterogeneity and stratification, is discussed in a 1987 paper by Sorbie et al. [4]. The paper re-confirms the results of previous studies which state that “the gas phase first occupies the high permeability strata and bypasses the low permeability zones (as a result of channeling), while the water phase flows into lower permeability zones which are not accessible by gas” [3]. An older study by Bunge and Radke [17] observed higher oil recovery in highly stratified reservoirs, where those reservoirs with minimal vertical transmissibility performed best. Keeping this in mind, it may become relatable to the Low Quality (LQ) reservoir for this simulation study. The low-quality reservoir has the lowest vertical-to-horizontal permeability ratio compared to the High Quality (HQ) and Ultra-high Quality (UHQ) reservoirs; however, none of the three reservoir sector models include any significant intra-flow unit stratification.

Moving on, relative permeability and hysteresis are discussed in the 1998 paper by Christensen et al. [15] where implementing a hysteresis relative permeability model for simulation tends to provide the most accurate view of subsurface phase behaviour during WAG. In 2003, Element et al. [18] published a paper concluding that hysteresis cycles are irreversible. As explained by Afzali et al., "the gas trapping by water leads to a reduction in the residual oil saturation; and both water and gas permeability values reduce. Thus, the fractional flow varies with the trapped gas saturation..."[3]. Overall, these comments indicate that, if possible, it is best to include hysteresis in any relative permeability model for a reservoir that uses WAG injection.

On the topic of wettability, Huang and Holm concluded that through WAG injection, oil trapping occurred mostly in water-wet rocks [3], [19]. This in itself suggests that WAG is

a more efficient process, for oil recovery, in mixed-wet to oil-wet scenarios. Afzali et al. cite several more detailed examples that also support this conclusion.

Several papers touch on the topic of most beneficial injection gas for gas flood and WAG. In a 2012 paper, Srivastava noted that CO_2 WAG yielded a ~40% increase in displacement efficiency over water flood, compared to a ~24% increase over water flood using produced hydrocarbon WAG [20]. The CO_2 gas likely has better miscibility with crude oil at reservoir conditions [20]. Common concerns with CO_2, such as; production system material compatibility and injectivity loss, can now be largely designed for and modelled in advance of implementation. If CO_2 is available, it is a possibility worth evaluating.

Injection cycles have become one of the most sensitized topics related to WAG depletion planning given the ease of analysis using modern simulation tools and uncertainty analysis. Afzali et al. conclude that a WAG schedule ratio of 1:1 is preferred and generally results in optimal recovery, and that the injection ratio has minimal impact in mixed wettability systems [3]. Further to this, tapering the WAG injection ratio late in life can reduce excessive gas production and prolong the life of the well or field, and potentially accelerate the oil front reaching the production wells [3]. This can be further flushed out via deterministic simulation cases, or if resources allow, a dynamic uncertainty model.

2.4.2.2. Core Scale Analysis

M.M. Kulkarni and D.N. Rao have done extensive work investigating the effects of immiscible gas flood and WAG through which they determined that the two methods had an insignificant effect on recovery [21]. Their latest paper from 2005 investigates the effects of using miscible gas flood and WAG for secondary or tertiary recovery through core-flood experiments conducted at various laboratory conditions using water-wet Berea sandstone [22]. This summary will focus only on the miscible, secondary recovery results and conclusions.

The results from miscible secondary gas flood indicate high oil recovery factors around 85% of the flooded core OOIP, low water production, and gas breakthrough occurring around 0.5 pore volume injected (PVI), with a trend of increasing gas production while oil production decreases [22]. Note that high Gas-to-Oil Ratios (GOR's) can be a significant limiting factor for production wells given operational constraints attributed to gas handling and processing equipment capacities. Due to this, high GOR's can lead to earlier than predicted shut-in of oil production wells and should be closely monitored.

On the other hand, the miscible secondary WAG flood resulted in even higher recovery, around 96%, combined with zero water production until gas breakthrough [22]. With the WAG experiment, the gas breakthrough occurred at 0.51 PVI while the water breakthrough occurred at 0.89 PVI [22], at which time most of the oil had already been produced which means water cut was not of great concern. Once the alternating injection had occurred for some time, after the first 2-3 slugs, the core entered into a three-phase

flow regime [22]. This flow was observed by periodic fluctuation of the measured pressure, depending on the injection fluid, and can be viewed as a positive given that there is no significant impact on flow behaviour. The result is beneficial by lowering drawdown and increasing fluid injectivity [22].

The paper concludes by noting the benefits of both secondary recovery methods with WAG results showing higher gas utilization factors than gas flooding [22]. In other words, the injected gas results in more beneficial recovery in the WAG cases. Additionally, the experimental results also suggest that any “extra” water injection could be more detrimental to secondary oil recovery than to tertiary recovery [22].

2.4.2.3. Machine Learning

Research by Belazreg et al. highlights machine learning and the development of a predictive model for WAG recovery based on a two-step approach of reservoir simulation and data mining [23]. For this research, one thousand dynamic reservoir models, with a range of input parameters, were simulated [23]. The results fed into two selected data mining techniques, regression and group method of data handling (GMDH), in order to build a predictive model for WAG recovery [23]. Ultimately, the GMDH technique prevailed while using 70% of the input data for machine learning, and 30% for validation purposes [23].

The initial reservoir simulation indicated that decreasing the WAG cycle length improves injected fluid mobility and sweep efficiency, and increasing the WAG ratio to favor gas injection, yielded accelerated recovery [23].

For example, a short WAG cycle for a large development may be considered 2 months, which is a common starting point for most development scenarios. A high WAG ratio may be considered 1:5, water to gas [23]. Using more gas will accelerate production as stated above but it will also lead to rapid gas breakthrough and early shut-in due to high GOR if unchanged.

Understanding the impact of the injection ratio and the well spacing will allow for flexibility in reservoir management with WAG. Production and injection wells that are spaced relatively close together will likely see breakthrough occur faster than wells spaced farther apart. In addition to well spacing considerations, decreasing the WAG injection ratio as gas breakthrough occurs will slow the increase of the produced gas-to-oil ratio. In another cited paper [3] this reservoir management technique of decreasing the gas injection cycle duration and increasing the water injection cycle duration was referred to as ‘tapering’.

The remaining simulation conclusions echo points that have already been discussed; such as, WAG incremental recovery over water flood ranges from 5% to 15%, WAG ratio should be changed periodically to delay rapid gas onset, and hysteresis is an important consideration to implement if possible [23].

Regarding the data mining aspects, the GMDH technique “has shown strength and ability in selecting the effective input parameter, optimizing the network structure, and achieving predictive model with high accuracy” [23]. These results indicate that this may lead to a very useful tool for future evaluations.

2.4.3. Effects of Hysteresis

The 1998 paper by Christensen et al. documented the testing of hysteresis in a simulation environment [15]. Using hysteresis with a compositional fluid model resulted in several issues around increased run-time; however, several runs were completed and it was concluded that applying two-phase hysteresis had no impact on the dynamic fluid interactions, resulting in no changes to sweep efficiency or recovery improvements [15]. Using a black oil fluid model allowed for additional testing of the relative permeability models, where, recovery was improved by implementing three-phase hysteresis. This improvement is due to delayed breakthrough of the gas phase, attributed back to a reduced gas relative permeability in three-phase areas of the model [15].

Afzali et al. [3] stress the importance of implementing drainage and imbibition processes into dynamic numerical models so that three-phase hysteresis effects can be accounted for, increasing the oil mobility, decreasing gas mobility, and resulting in more realistic predictions [3]. Afzali et al. further elaborate that “[t]he relative permeability models become less accurate in near miscible conditions when the mass transfer between the two phases occurs” [3] so this provides one potential exception; however, it would be best practice to test the simulation with and without hysteresis.

A recent study conducted by Kowsari et al. evaluated “The Effect of Relative Permeability Hysteresis on the Design of an Optimal Water-Alternating-Gas (WAG) Process” [24]. Two reservoir models were used in this assessment, a benchmark homogeneous reservoir model and a more complex heterogeneous field-based reservoir model [24]. The researcher used a combination of Particle Swarm Optimization (PSO) and Evolutionary Strategy (ES) to optimize WAG parameters being used for the sensitivity analysis. From the results of the sensitivity analysis, Kowsari et al. concluded that WAG flood simulation cases may overpredict oil and gas production volumes, and underpredict water production volumes, in cases where no hysteresis model is active [24]. Further to this, the recovery factor was found to be a function of hysteresis model selection, and using an inappropriate hysteresis model could result in suboptimal WAG design which could in-turn underpredict recovery factor by as much as 8% [24].

With today’s enhanced computational abilities, it is certainly worthwhile to test the effects of three-phase WAG hysteresis with a compositional fluid model and, preferably, a full-field or sector development model.

2.5. Summarized Literature Findings

1. WAG is gaining traction as a secondary recovery method for offshore applications where the ability to dispose and recycle excess gas alleviates environmental and economic concerns [14]. Field gas injection requirements create an opportunity for WAG as it requires less gas than gas flood to achieve an effective reservoir sweep and is generally more efficient [11], [14].
2. WAG is most beneficial in oil-wet to mixed-wet systems given that it may induce oil trapping in water-wet systems [3], [19].
3. WAG increases recovery factor by 5% to 15% compared to water flood [3], [14], higher than the increase observed using gas flood [15]. Compared to water flood, a mean 10% increase in recovery factor is observed using miscible WAG and a mean 6% increase using immiscible WAG [14].
4. The gas-to-water injection ratio depends on reservoir characteristics. Lower permeability intervals are preferential for the water phase while higher permeability intervals are preferential for the gas phase [4], [25]. A schedule ratio of 1:1 is preferred throughout most of production; however, tapering gas injection during late-life is helpful to reduce excess gas production [3],[23].
5. Decreasing WAG cycle duration improves mobility and sweep efficiency [23].
6. Using a wet injection gas further improves WAG recovery [15].
7. Adding CO_2 to injection gas improves recovery. CO_2 induced corrosion concerns do exist and can be best mitigated during the design phase [14]. Compared to water flood, WAG with produced gas increases displacement efficiency (DE) by 24% and WAG with CO_2 increases DE by 40% [20].
8. Simulating two-phase hysteresis has minimal impact on phase behaviour and recovery [15]; however, simulating three-phase hysteresis does influence the gas relative permeability in three-phase areas and improves overall recovery [15]. Three-phase flow with water, oil, and gas becomes present after several initial slugs of the water and gas phases are injected [22].
9. Reservoir studies performed by Kowsari et al. indicate that WAG simulations without hysteresis (e.g. using only drainage curves) may overpredict oil and gas production volumes and underpredict water production volumes [24]. This is exemplified in Figures 1 and 2 from the paper by Kowsari et al. [24] where the imbibition relative permeability curves undercut the drainage curves. If the imbibition relative permeability curves are not implemented, then the resultant simulation will inherently over predict hydrocarbon production volumes by adhering to the higher relative permeability defined by the drainage curves. Using an inappropriate hysteresis model could result in suboptimal WAG design which could underpredict recovery factor by as much as 8% [24].
10. Core flood studies suggest that secondary gas flood and WAG cases observe gas breakthrough at 0.5 PVI and water breakthrough at 0.9 PVI [22].

3. Methodology

3.1. Geological Sector Models

3.1.1. Derivation

Three sector models have been created by extracting sections of reservoir from various full field development models. These full field models have been constructed using a combination of seismic response, well log response, and laboratory data acquired from experimental analysis of core and fluid samples taken from exploration and appraisal wells in the Flemish Pass Basin. The full field development models inherently contain a high degree of geological complexity while maintaining the geological and fluid characteristics observed in regional exploration wells. As a result of these models sampling various geological and depositional environments, the three sector models represent a discrete range of different quality reservoirs. The models represent Ultra-High, High, and Low-quality reservoirs. This approach is drastically different and more representative of actual reservoir conditions than a simplified box model would be. Taking this approach allows for the simulation study to be highly analogous to the real-world discoveries upon which the models are based.

For example, even though the highest quality sector model may have significantly lower connate water saturation and significantly higher porosity and permeability than another sector model, the physical dimensions of both reservoirs are kept to the same scale such that they maintain relatively similar physical dimensions and can be developed with similar depletion plans (e.g. well spacing, well length)

The three sectors have been defined within the available static field development models by an ‘ACTNUM’ or region of active cells property. The three ACTNUMs, representing the three sector models, have relatively similar lateral and depth dimensions in order to provide consistency across the simulation cases. The sectors are used as the geological basis for this research and represent different levels of reservoir quality, defined locally as Ultra-High-quality, high-quality, and low-quality reservoirs. The nomenclature is relative to geological quality discovered in wells Offshore Atlantic Canada, specifically in the Flemish Pass Basin. Note that all well results, including reservoir quality, are publicly available through the C-NLOPB [7] and Natural Resources Canada BASIN [26] websites.

3.1.2. Model Summary and Parameters

In the following tables, the mean geological and initial fluid properties are defined for each of the three sector models. Note that the tabulated values only represent the statistical mean value for the filtered cells of each sector model. These values are not representative of the entire development model, specific discovery wells, or core analysis results. The fully representative well data sets can be accessed from the C-NLOPB website [7].

The mean sector dimensions have been identified in the tables below by measuring each sector model at specified points and averaging those measurements. The specified measurement points are:

- North-to-South along Western extent, Eastern extent, and center line
- East-to-West along Southern extent, Northern extent, and center line
- True Vertical Depth: Five measurements at the four extents and center point of each sector

For each of the following data tables, two screen captures with 2.0 vertical exaggeration are included to provide the reader with a visual understanding of the facies distribution, degree of intra-block faulting, and modelled geological complexity. For the facies nomenclature, the following acronyms are used:

- Mg-Cg Sandstone: Medium Grain to Coarse Grain Sandstone
- Fg Sandstone: Fine Grain Sandstone
- Slt-Vfg-Fg Sand: Siltstone to Very-fine Grain to Fine Grain Sandstone
- Mg-Fg Sandstone: Medium to Fine Grain Sandstone
- VFg Sandstone: Very-fine Grain Sandstone

All three sector models are considered to be of mixed or neutral wettability.

The following table outlines the mean parameters for the three different quality reservoirs. The tabulated values only represent the filtered statistics for each sector model and do not represent the full-field development models.

Table 1: Mean Sector Model Parameters

Mean Sector Model Parameters	Ultra-High-Quality	High-Quality	Low-Quality
Horizontal Permeability (mD), Sandstone	3,840	1,608	166
Vertical to Horizontal Perm. (Kv-Kh) Ratio	0.7	0.7	0.4 to 0.7 porosity dependent
Porosity (%), Sandstone	25.2	21.6	20.4
Pore Volume (Rm3)	4,599,826	3,105,439	1,868,623
Connate Water Saturation (%), Sandstone	8.9	15.3	14.0
Lateral Dimensions (m)	~1,000 x 1,000	~1,300 x 1,300	~1,000 x 1,000
Thickness (m TVD)	~20	Varies, ~5 to ~15	~20
Sector Model Dip Angle	Medium	High	Low
Cell Dimensions (m)	50 x 50 x 1	50 x 50 x 1	50 x 50 x 1

UHQ Model **Permeability** **Segments with Well Pair**

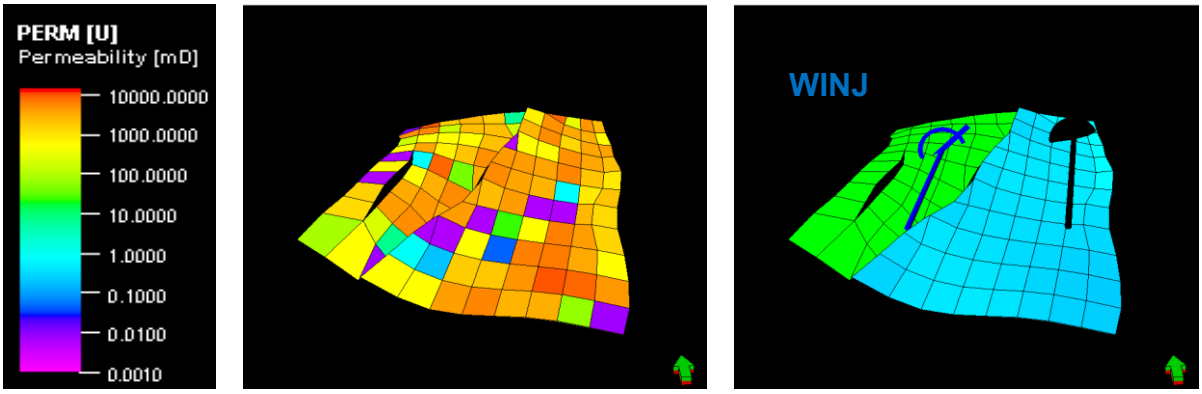

Figure 5: Ultra-High-Quality Sector Model, K-Slice

HQ Model **Permeability** **Segments with Well Pair**

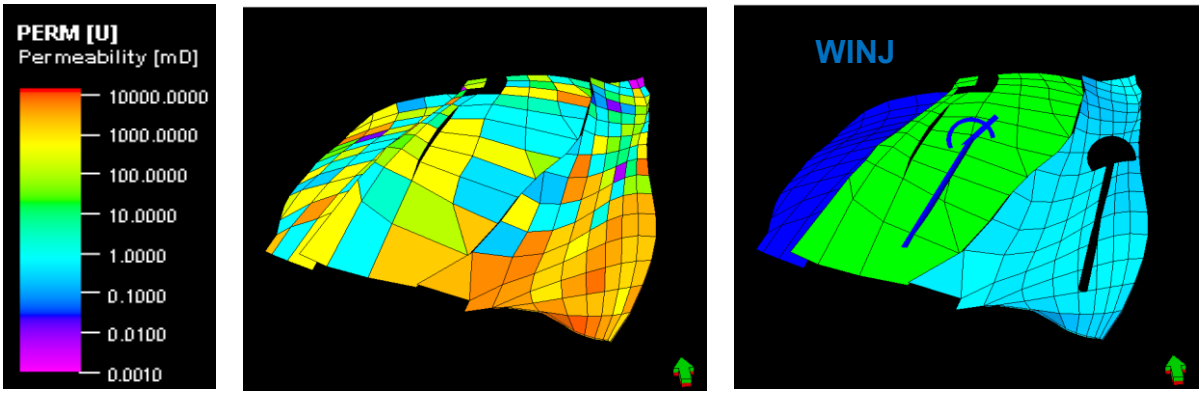

Figure 6: High-Quality Sector Model, K-Slice

LQ Model **Permeability** **Segments with Well Pair**

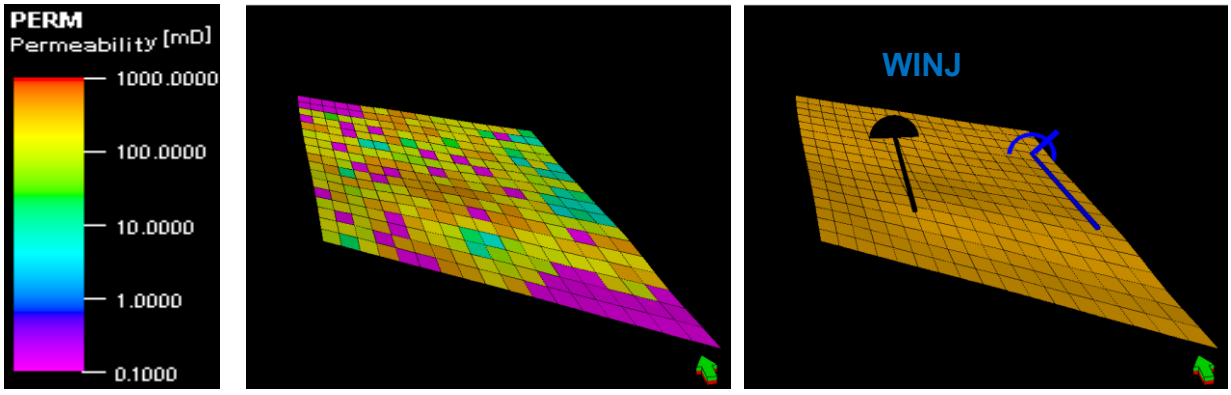

Figure 7: Low-Quality Sector Model, K-Slice

3.2. Fluid Data and Characteristics

This study utilizes two fluid models that represent a light, sweet crude around 36 °API and a medium, sweet crude around 21 °API. Both fluids are modelled based on multiple downhole samples, extracted from exploration wells in the Flemish Pass Basin. Both oils originated from very undersaturated reservoirs with low to moderate gas-in-solution. For water, the salinity is considered to be static for the purpose of this study, around 33,000 ppm NaCl. Figure 8 below highlights the compositional consistency of the light oil samples, displayed in light grey, with the representative light oil sample overlaid in red. The medium oil sample is displayed in blue and, as expected, has much higher mole fractions for the C12+ components compared to the representative light oil sample.

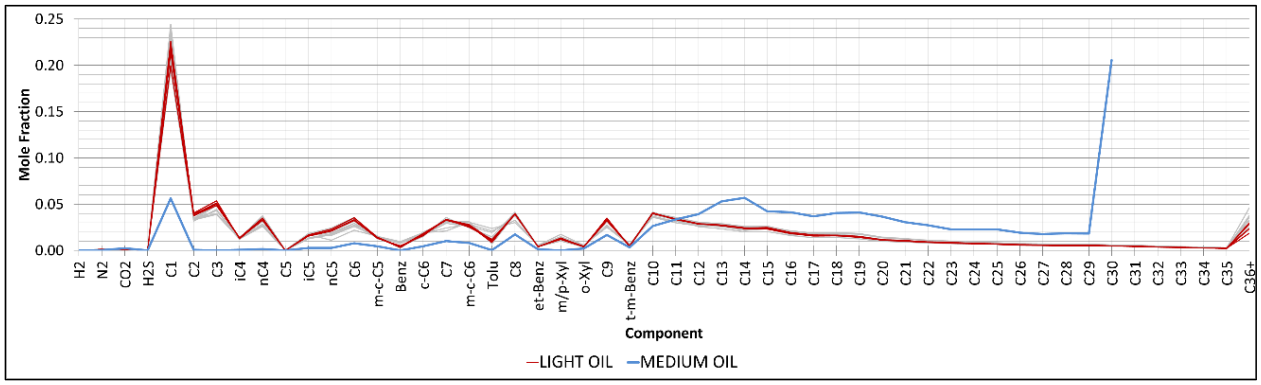

Figure 8: Composition Chart for Light and Medium Oil Samples

3.2.1. Light, Sweet Oil (36 °API)

Five samples extracted from the Ultra-High-Quality reservoir within 'Development Area A' are utilized in the light oil fluid model. An analysis of the compositional data, shown in Figure 8 above, indicates consistent compositions and characterization parameters between the five selected samples which are indicated by grey lines behind the red line. The red line indicates the selected sample composition that is exported for simulation to represent the light oil model.

This oil was sampled in several exploration and appraisal wells. The study focuses on five of the samples that underwent the most impactful PVT experiments and also show a high degree of compositional consistency. Observe from the data in Table 2 that the Light Oil samples come from a high pressure, undersaturated reservoir with fairly low GOR. The reservoir pressure is around 380 bar with a saturation pressure around 75 bar, and GOR ranging from 45 to 55 Sm^3/Sm^3.

Table 2: Tabulated Overview of Light Oil Sample Properties

Well	Sample	Reservoir	Density (g/cm^3)	Density (°API)	GOR (Sm^3/Sm^3)	T-res (°C)	P-res (bara)	P-sat (bara)	Bo (Rm^3/Sm^3)	Viscosity (cP)	Salinity TDS (mg/L)
01											33,500
	A	UHQ	0.845	36.1	53.0	77	381	81	-	1.30	
	B	UHQ	0.848	35.5	52.5	78	384	81	1.15	1.21	
02											34,600
	A	UHQ	0.844	36.1	55.6	79	385	82	1.15	1.05	
03											32,400
	A	UHQ	0.843	36.3	47.9	76	378	77	1.13	1.25	
	B	UHQ	0.847	35.6	52.7	76	379	70	-	-	
Density and GOR are reported at Stock Tank Conditions of 1.016 bara and 15.6 deg C.											

3.2.2. Medium, Sweet Oil (21 °API)

The medium oil is to be based on a downhole sample that was only sampled in a single exploration well; however, due to the potentially commercial volumes, characterizing the phase behaviour of this particular oil is becoming an increased focus. In the Offshore Atlantic region, operators are not accustomed to dealing with this relatively heavier oil, so it does become a Reservoir and Production engineering challenge to effectively sweep and produce. Observe from Table 3 that this reservoir is also at a high pressure, with a relatively higher temperature, 380 bar and 90 degrees Celsius, and a saturation pressure around 19 bar which means the reservoir is very undersaturated. The Solution Gas-to-Oil Ratio is around 5 Sm^3/Sm^3, making this effectively a dead oil.

Table 3: Tabulated Overview of Medium Oil Sample Properties

Well	Sample	Reservoir	Density (g/cm^3)	Density (°API)	GOR (Sm^3/Sm^3)	T-res (°C)	P-res (bara)	P-sat (bara)	Bo (Rm^3/Sm^3)	Viscosity (cP)	Salinity TDS (mg/L)
01											36,000
	A	HQ	0.927	21.1	4.6	91	381	19	1.02	12.80	
Density and GOR are reported at Stock Tank Conditions of 1.016 bara and 15.6 deg C.											

3.3. Fluid Modelling

3.3.1. Light, Sweet Oil (36 °API)

The five original compositions representing the fluids used for laboratory experiments are input in the PVT modelling software, Calsep PVTSim. These compositions are then used to simulate the experiments and are regressed to the true lab results. The goal is for the simulated experimental results (from composition) to match the true lab results as best possible for each of the fluid parameters.

The steps below outline this process.

1. Five compositions are tuned to a 'Common Equation of State (EoS) w/ Plus Regression', equally weighed with all experiments enabled for the initial tuning step.
    - Peng Robinson EoS model
    - Temperature dependent Peneloux density correction to improve density alignment
    - Lohrenz-Bray-Clark (LBC) viscosity model
    - Modified lumping scheme as per Figure 9

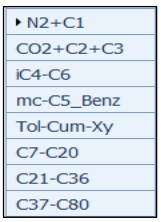

Figure 9: Light Oil Lumping Scheme

2. Next, each sample with true lab data is evaluated based on how closely their lab results align with the simulated results generated from the fluid's composition.

   The parameters with the best alignment (lab vs. simulated) are selected for further regression. The selected parameters are noted in Table 4 below.

Table 4: Selected Light Oil Experiments for Plus Regression

Well	Sample	Experiment	Selected Parameters
01	A	CME	Compressibility
01	B	DLE	All
02	A	CME	Y-Function, Density
	A	Sep. Test	All
	A	Viscosity	All
03	A	None	
03	B	CME	Relative Volume

3. Following step two, a new iteration of the '**Common Equation of State (EoS) w/ Plus Regression**' tuning process is conducted using the fluid samples from step one and the selected parameters from step two, as noted in Table 4.

   For example, the first row of data in Table 4 details Well 01, Sample A. For Well 01, Sample A, the experimental data from the Constant Mass Expansion experiment is used for plus regression; however, only the Compressibility parameter receives a weighing value of 1 while the other results (e.g. Relative Volume) are assigned a weighing value of 0. This weighing is assigned based on the selected parameters from step two.

   The result of this process is a preliminarily tuned fluid model with simulated fluid characteristics that are similar to the true laboratory results.

   The parameters inherent within this preliminary fluid model are displayed in each of the following plots in Figure 10.

   Observe how the green lines, representing the preliminary model, are now in better alignment with the experimental data (blue dots) than the initial model, represented by the orange lines.

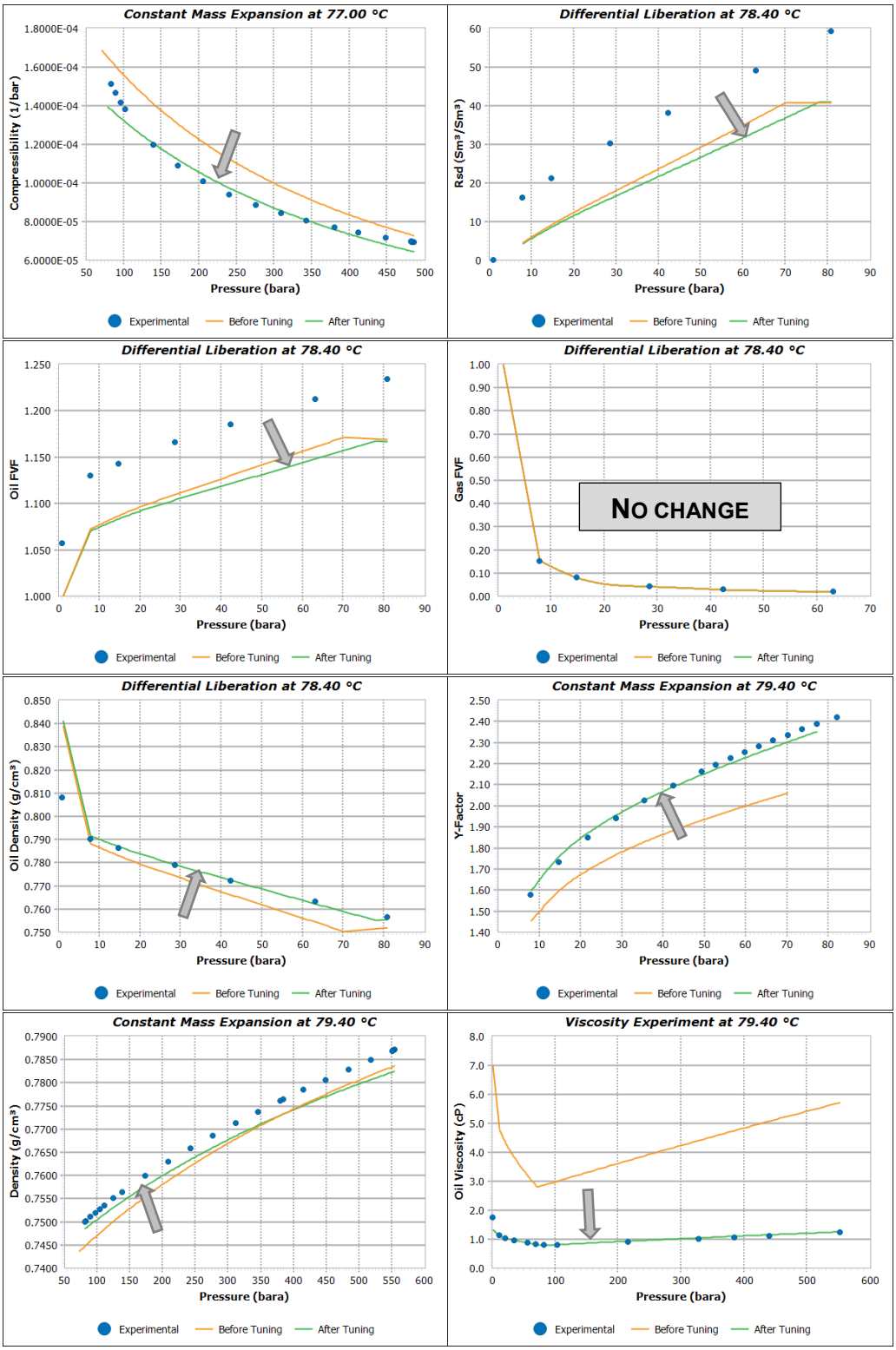

Figure 10: Light Oil, PVT EoS Tuning with Plus Regression

4. Given that there is still room for improvement, for example, Oil Formation Volume Factor ('Oil FVF', also called 'Bo') and Solution Gas Ratio ('Rsd') are not well aligned, the next step is to perform a '**Common EoS with Characterized Regression'**. The characterized regression process is displayed in Figure 11.

   During this process, the preliminary Plus Regressed model will be further improved by characterized regression.

   The weights of the 'Oil FVF' and 'Rsd' parameters are increased to improve their alignment with the true lab data. In other words, more emphasis is placed on matching the 'Oil FVF' and 'Rsd' parameters than the other parameters.

   On top of the changes to parameter weighing, additional flexibility is allowed between the various lumped component parameters, such as Critical Temperature, Critical Pressure, Acentric Factor, Molar Critical Volume, Omega A, Omega B, and the volume shift parameter. Added flexibility is also specified between the binary interaction coefficients for each of the lumped components.

   This flexibility is allowed via specific user-input ranges. The PVT software further regresses and ultimately generates a tuned fluid model via characterized regression. After multiple iterations or attempts at this process, a fluid model that is better aligned with the experimental data should result. In this case there are two parameters, specifically 'Oil FVF' and 'Rsd', that are focused on. The resultant characterized fluid model is improved and is then output for use in the dynamic model or reservoir simulator software. The final characterized fluid model results are displayed in each of the following plots. Observe the solid green lines representing the final tuned model. These plots demonstrate better alignment with the true lab data, plotted as blue dots. Note that the X and Y scales are set to 'auto-scale' and may be slightly different than those in the plus regressed fluid model plots. For those viewing this paper in black and white, arrows have been annotated on each plot to show the progression from preliminary to final fluid model. The 'Error Sum of Squares' or SSE is annotated on each chart to provide insight into regression success.

5. The final fluid model is exported in the format of an Eclipse 300 compositional 'PROPS' include file and is then incorporated into the simulation case.

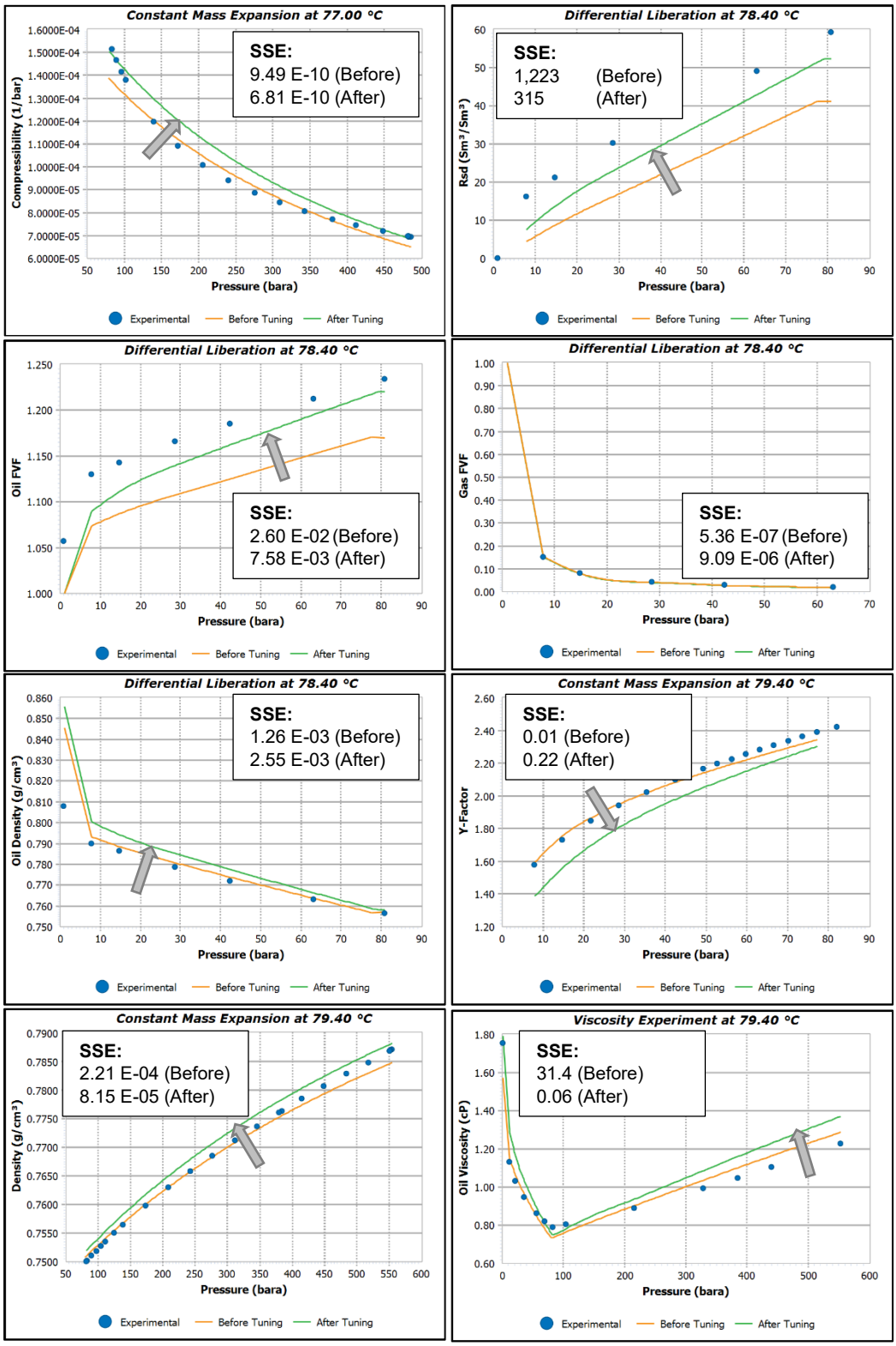

Figure 11: Light Oil, PVT EoS Tuning with Characterized Regression

3.3.2. Medium, Sweet Oil (21 °API)

The modelling process for medium oil follows the same process described for the light oil. Given that there are no major changes to the process, only the final tuned model parameters and notes regarding the sample are detailed below.

The medium oil was sampled from a different field, approximately ~40 kilometers away. The sampled well was drilled with oil-based mud and underwent a drill stem test (DST).

The well was not cleaned up sufficiently; therefore, all collected fluid samples were moderately to highly contaminated with OBM. The samples contain very low gas-in-solution (Rs) therefore no samples were taken from the test separator during the DST.

Bottom hole MDT samples were collected but contaminated with 17 wt% to 35 wt% OBM. Basic Sediment & Water (BSW), essentially water content, measured around 10%. Very low 'Rs' measured between 2.3 – 3.8 Sm^3/Sm^3. The reservoir was determined to be very undersaturated with a bubble point pressure (P_b) between 16.2 and 18.6 bara and a reservoir pressure (Pr) between 381 and 382 bara. The sampled fluids measured between 22.0 and 22.6 °API. Unfortunately, the laboratory did not correct these MDT fluid samples for the OBM contamination and did not use these samples for any experiments.

Bottom hole DST samples were also collected, and these were determined to be contaminated with 2.5 wt% to 9.0 wt% OBM. BSW, water content, measured between 4% to 10%. The sampled DST fluid measured roughly 21.1 °API.

In order to properly analyze this fluid, the lab needed a water free and decontaminated sample so oil from the DST sample was flashed and dried, then recombined with gas to correct the fluid to estimated reservoir conditions. The laboratory proceeded to use this recombined DST fluid for experimental analysis.

Differential liberation and constant mass expansion experiments were performed and are used as the basis for plus regression and characterized regression. In this case, only the one sample was tested therefore this is not considered a 'Common EoS'.

Model parameters:

a. Peng Robinson, predictive 1978 EoS model
b. Temperature dependent Peneloux density correction
c. Lohrenz-Bray-Clark (LBC) viscosity model
d. Modified lumping scheme as per Figure 12.

Component
N2+C1
CO2+C2+C3
iC4-C6
C7-C24
C25-C43
C44-C80

Figure 12: Medium Oil Lumping Scheme

Refer to charts outlining the final parametric adjustments in Figure 13 on the next page.

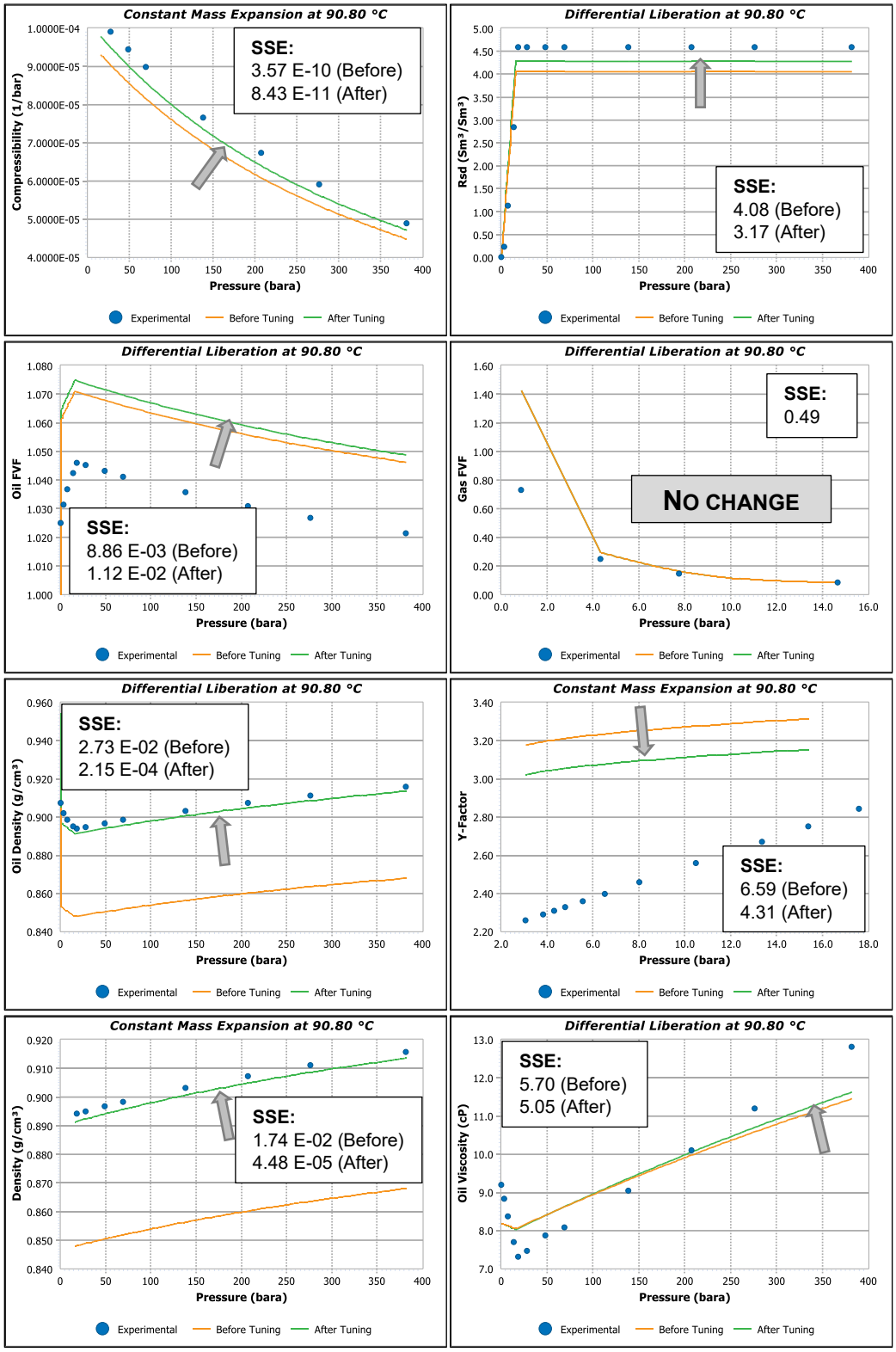

Figure 13: Medium Oil, PVT EoS Tuning with Characterized Regression

3.4. Additional Dynamic Model Inputs

3.4.1. Water Saturation Models (J-Function)

The water saturation models populate the initial water saturation value for every active cell in the simulation model at the first-time step. The hydrocarbon phase saturations are back-calculated based on these initial water saturation values. Several of the relative permeability saturation endpoints, such as connate water saturation (S_{wc}), also referred to as irreducible water saturation, and the critical oil-water saturation (S_{owc}), also referred to as the residual oil saturation, also play a role in dictating the initial saturation values of each cell.

This section will provide an overview of how the water saturation models are derived and how they compare to one another. The next section will evaluate the relative permeability endpoints and curves.

The saturation models are based on the Leverett J-Function [27] and derived from Special Core Analysis (SCAL) experimental results obtained from laboratory analysis. The experiments are conducted on conventional core samples from various exploration and appraisal wells. In particular, capillary pressure (P_c) test results are used to derive the Water Saturation models.

These capillary pressure tests are conducted with any of three common methods, Centrifuge, Porous Plate, or Mercury Injection. The fastest and most expensive method uses the Centrifuge, which is the method used for testing these specific core samples.

Results are provided from the laboratory for primary drainage at nine pressure stages. These results are denormalized and are representative of laboratory conditions, not reservoir conditions. Given this, the derivation procedure is followed to convert the laboratory capillary pressure curves to a dimensionless Leverett J-Function curve at reservoir conditions.

1. Convert Pc data at laboratory conditions to reservoir conditions using the measured interfacial tension (σ) and contact angle (θ) at laboratory conditions, and estimated σ and θ at reservoir conditions. If the reservoir σ and θ values are unknown, SCAL ambient interfacial tension experiments can also be conducted by the laboratory to determine these. As an alternative, σ at reservoir conditions can also be estimated based on fluid composition and phase densities.

$$\frac{P_{c(lab)}}{\sigma \cos\theta_{(lab)}} = \frac{P_{c(res)}}{\sigma \cos\theta_{(res)}}$$

Equation 1: Capillary Pressure conversion between lab and reservoir conditions [28].

Units are bara for capillary pressure (P_c), dynes/cm for interfacial tension (σ), and degrees (°) for contact angle (θ).

2. Convert Pc curves at reservoir conditions to J-Function curves using the measured permeability and porosity for each of the tested core samples and the associated σ and θ values.

$$J = 0.0314 \left(\frac{P_{c(res)} \sqrt{\frac{k}{\emptyset}}}{\sigma \cos \theta_{(res)}} \right)$$

Equation 2: Dimensionless Leverett J-Function describing Capillary Pressure [27].

Units are bara for capillary pressure (P_c), dynes/cm for interfacial tension (σ), degrees (°) for contact angle (θ), millidarcy (mD) for permeability (k), and dimensionless for porosity (∅) where porosity is reported as a fraction between 0.0 and 1.0.

3. Normalize each J-Function curve based on the water saturation values, where 'S_{wc}' is the minimum value of S_w reached during the primary drainage experiment.

$$Sw^* = \frac{(Sw - S_{wc})}{(1 - S_{wc})}$$

Equation 3: Normalization of Water Saturation to Connate Water Saturation endpoints [28].

Water saturation (S_w) is dimensionless, reported as a fraction between 0.0 and 1.0.

4. Scale each of the normalized J-Function curves so that they are tied to a maximum hydrocarbon column height or 'Height Above Free Water Level' (HAFWL). The maximum column height is based on the contact depths.

   In the equation below, the change in density is based on the differential between the phase densities, for example, the difference between the oil density and water densities in kg/m^3.

$$HAFWL = \frac{P_{c(res)}}{0.00981\left(\rho_{(water)} - \rho_{(oil)}\right)}$$

Equation 4: Conversion from Capillary Pressure to 'Height Above Free Water Level' [28].

Units are meters true vertical depth subsea (m TVDss) for Height Above Free Water Level (HAFWL), bara for capillary pressure (P_c), and kg/m^3 for the phase densities (ρ).

5. Once a normalized grouping of J-Function curves has been scaled to a uniform maximum HAFWL, the curves can be evaluated, and outlier curves can be removed from the analysis if sufficient reasons exist.

   The final group of J-Function curves are plotted together, and a best fit equation must be determined to represent a best fit curve through the grouping. There are several software packages available to conduct this curve-fitting procedure.

   This best fit equation is applied to a range of water saturation values from 0% to 100% (0.0 to 1.0). This equation represents the final J-Function curve which then acts as the normalized Sw input for the dynamic model. This function is called upon to populate each model cells' saturation values at the initial timestep. The curve can be shifted depending upon permeability and associated connate water saturation (Swco) endpoints for various bands of permeability.

Having completed this derivation, the final J-Function curves are plotted in Figure 14 below. Each curve represents the water saturation function that is used to populate the dynamic model cells with an initial saturation value. Each cell in the model is determined to be at a specified height above the free water level or HAFWL. This HAFWL corresponds to a dimensionless J value and to an initial water saturation value depending upon its position along one of the representative curves outlined in Figure 14. The curve or bin that each cell is assigned to depends upon the cell's horizontal permeability value.

Saturation functions for the Ultra-High-Quality and High-Quality sector models are segregated into four sandstone permeability bins. The bins are generated based on data from Routine Core Analysis (RCA) and Special Core Analysis (SCAL).

1. $K_h > 2{,}000$ mD — $S_{wc} = S_{wc1}$
2. $2{,}000 \geq K_h > 300$ mD — $S_{wc} = S_{wc2}$
3. $300 \geq K_h > 10$ mD — $S_{wc} = S_{wc3}$
4. $K_h \leq 10$ mD — $S_{wc} = S_{wc4}$
5. Other Facies — $S_{wc} = 1.00$

The Low-Quality reservoir is represented by a single S_{wc} value and is not varied by permeability. This is supported by a much narrower range of permeability encountered in the Low-Quality reservoir.

1. All Sandstone, All K_h — $S_{wc} = S_{wc5}$
2. Other Facies — $S_{wc} = 1.00$

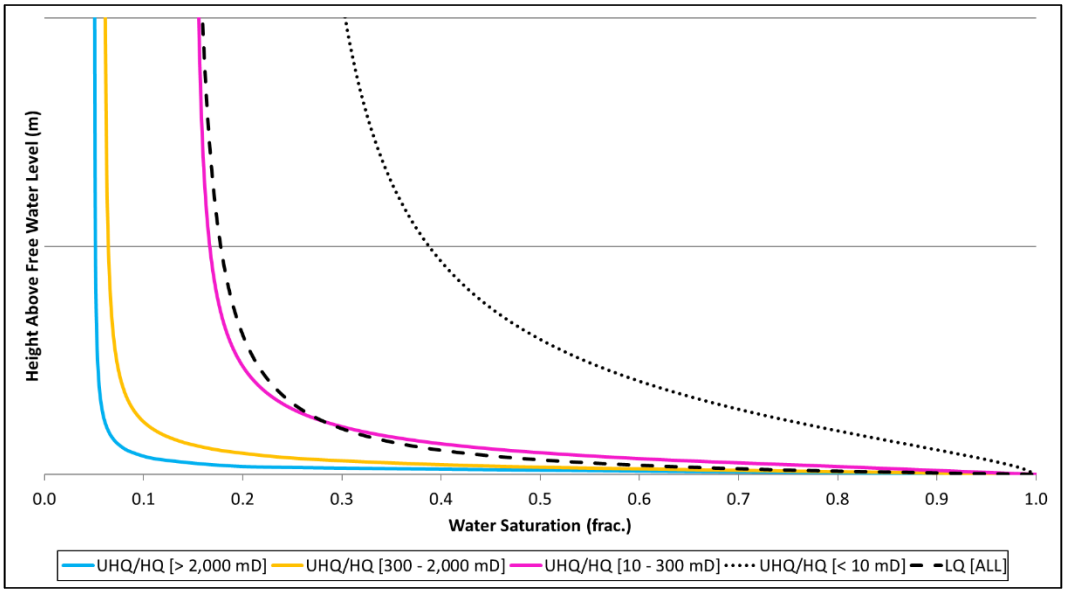

Figure 14: Water Saturation (J-Function) Models

3.4.2. Relative Permeability Models (LET Method)

The relative permeability models are derived from SCAL lab results. The curves and endpoints are based on steady state oil-brine and gas-oil experiments conducted on conventional core extracted from regional exploration wells. In addition to the SCAL results, catalogued global data from analogous offshore fields are also weighed to fine-tune the relative permeability models. This analogous data is used to supplement the relatively little data available from the Flemish Pass, given a limited number of well penetrations.

The models are generated using a LET correlation method [29] where each section of the relative permeability curve is designated with a variable (L, E, T) that reflects the magnitude of curvature and point of curvature. Figure 15 helps visualize the influence of each LET variable.

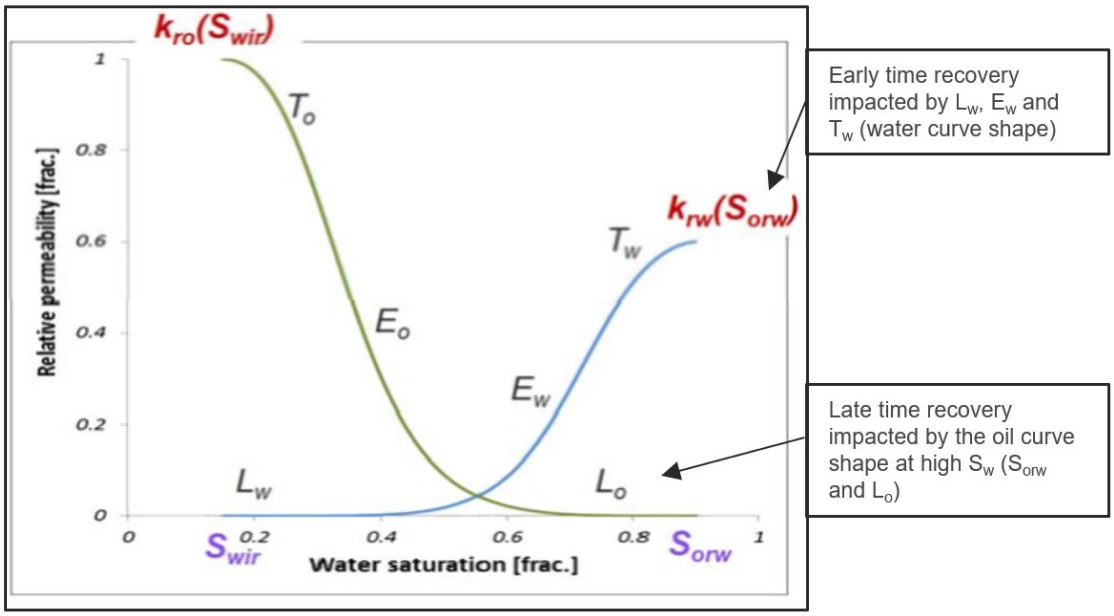

Figure 15: Generic water-oil curves influenced by LET parameters (Equinor ASA, 2017)

The final set of oil-water and gas-oil curves are shown in Figure 16 through Figure 19 on the next page. The ultra-high-quality and high-quality sector models use the same set of curves given that the SCAL results represent a combination of core samples from both reservoirs. The low-quality sector model has its own set of curves based on separate SCAL results from an appraisal well in that reservoir.

The curves are input in the dynamic model as normalized and then scaled to their respective endpoints. This is known as 'endpoint scaling'. Both normalized and denormalized curves are shown to emphasize the impact of the endpoint values.

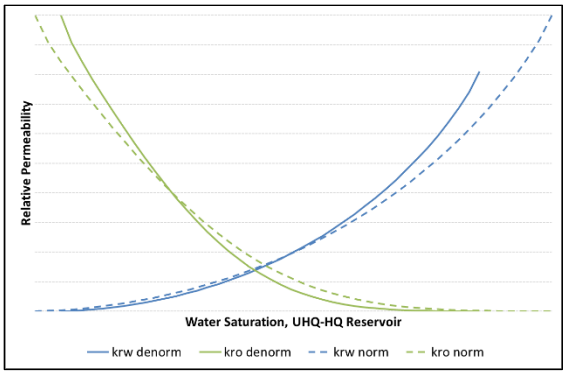

Figure 16: UHQ-HQ Reservoir, Oil-Water Drainage Relative Permeability Curves

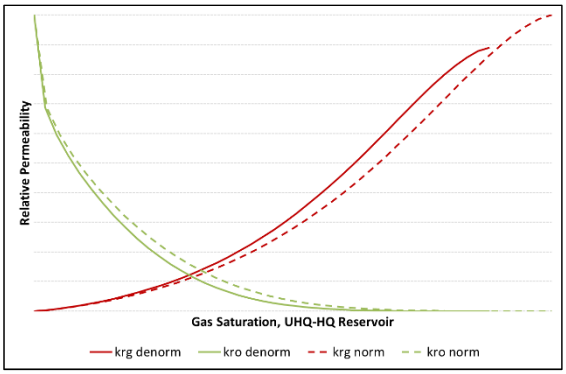

Figure 18: UHQ-HQ Reservoir, Oil-Gas Drainage Relative Permeability Curves

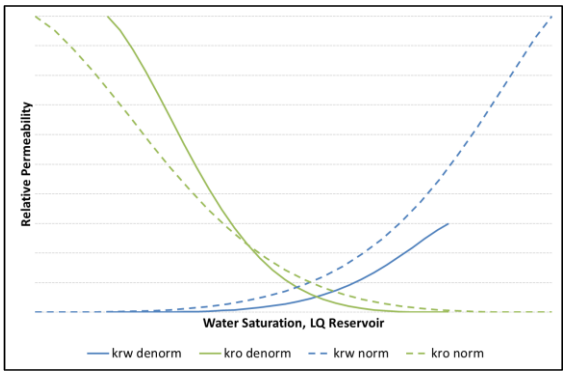

Figure 17: LQ Reservoir, Oil-Water Drainage Relative Permeability Curves

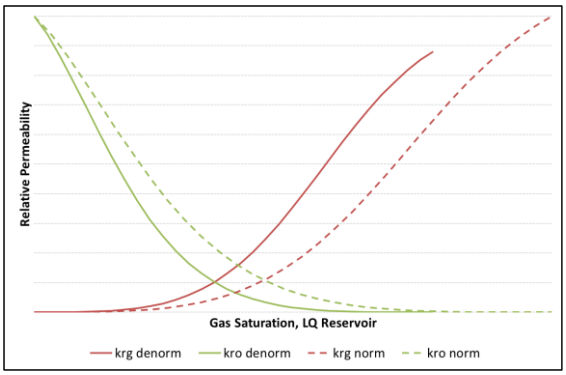

Figure 19: LQ Reservoir, Oil-Gas Drainage Relative Permeability Curves

The oil-water curves for both ultra-high-quality/high-quality and low-quality reservoirs indicate a mixed or neutral wettability system given that the crossover point of the denormalized curves falls near the 50% saturation mark in both. Keep in mind that Connate Water Saturation (S_{wc}) changes depending on rock permeability, so the curves translate depending on the permeability bin. Also observe that the Residual Oil Saturation from Water (S_{owcr}) ranges between 10% to 20% depending on the sector model.

3.4.3. Development Strategies

The study will utilize eighteen simulation cases to capture water flood, gas flood, and WAG flood depletion scenarios for each of the light oil and medium oil fluid models in the ultra-high-quality, high-quality, and low-quality reservoir sector models. Results will be analyzed by reservoir quality in relative context without use of explicit recoverable volumes.

The ‘Simulation Case Structure’ outlined in Figure 20 uses a sensitivity analysis experimental design in order to test the well pair recovery associated with each secondary oil recovery method. The recovery is to be tested using both light and medium oil fluid models, and three different quality reservoir models. The sensitivity analysis is broad, with the goal of determining which reservoir and oil observe the most benefit using the three recovery methods of water flood, gas flood, and WAG. As stated in the introduction, the three reservoir sector models and two fluid models are based on discoveries in the Flemish Pass Basin.

The simulation study focuses on five-year simulation cases where the impacts of each depletion strategy and oil quality are most obvious and influential. Additionally, extended duration cases were also completed. The intent of these extended duration cases is to specially focus on the recovery factor behaviour at high pore volume injected (PVI) ratios, equivalent to late production life. The longer duration cases are difficult to assess due to difficulties in maintaining realistic, extended well productivity in a small sector model and, in some occasions, needing to decrease the bottom hole pressure constraint in order to allow the well pair to continue flowing for an extended period. Some of these extended duration results will be discussed for the intended purpose of evaluating recovery at high pore volume injected ratios.

The WAG cycles operate using a simple control scheme of 2 months water injection followed by 2 months gas injection, with no variation. The cycle is based on common industry practice and discussed in relevant literature which suggests a 1:1 water to gas injection cycle ratio and low WAG cycle duration to improve mobility and sweep efficiency [3], [23]. The cycle duration of 2 months is relatively short in production time, and a cycle ratio of 1:1 water to gas is maintained. The sector model simulation cases assume access to produced solution gas from a full-field development where there is enough produced gas available for reinjection and adequate pressure maintenance. This applies to all WAG flood and gas flood sector model cases.

Many constraints are not explicitly stated given the confidential nature of ongoing development planning within the Flemish Pass and the use of reservoir sector models that have been extracted from actual full-field development models.

The bottom hole pressure limits are generally 70 to 100 bar below the initial reservoir pressure so that does provide some flexibility to draw down the well before having to reduce production flow rate. The maximum injection pressures are broadly based on cap rock integrity studies; however, non-field specific values are used for the purpose of this study.

The shut-in constraints are normally determined based on commerciality of the well; however, for this project, standard values or 'rules of thumb' are used to ensure an acceptable level of consistency between the simulation cases and their results. The maximum water cut is set to 95% and a minimum oil rate is based on a percentage of the maximum oil rate.

An additional goal is to maintain a miscible gas flood and miscible WAG flood. Given this strategy, the reservoir pressures will be maintained above minimum miscibility pressure for the duration of all studies.

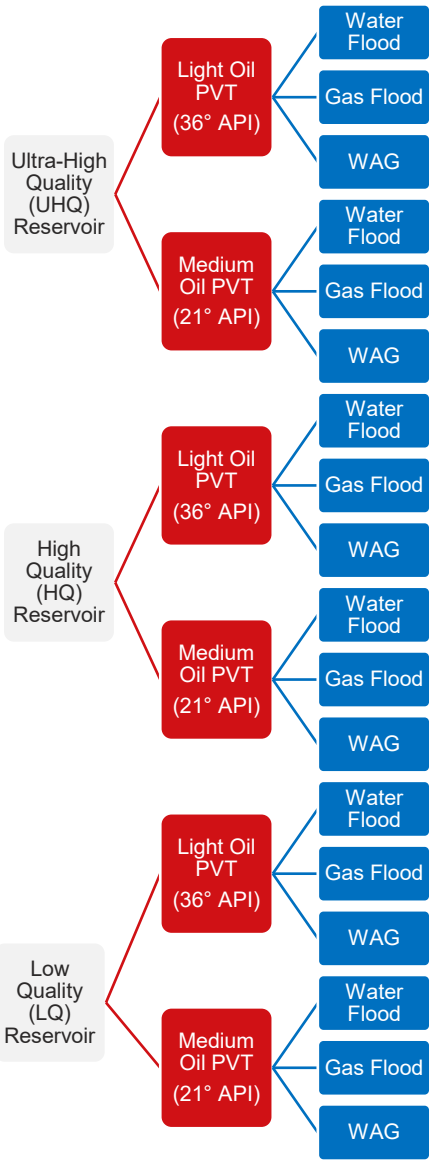

Figure 20: Simulation Case Structure

Ultra-High-Quality Reservoir:

Bottom hole Pressure:	310 bara (Min. Prod)
	450 bara (Max. Inj)
Shut-in Water Cut:	95%
Shut-in Min. Oil Rate:	75 Sm^3/d

High-Quality and Low-Quality Reservoir:

Bottom hole Pressure:	280 bara (Min. Prod)
	475 bara (Max. Inj)
Shut-in Water Cut:	95%
Shut-in Min. Oil Rate:	25 Sm^3/d

4. Results and Discussion

4.1. Overview

The eighteen simulation cases produce consistent and logical results that support the benefit of using WAG in all of the scenarios when quantified by recovery factor. This section will dive deeper into the results to evaluate which scenarios benefit the most from the various recovery methods, other variables for quantifying benefit of the recovery methods, and how production constraints may also factor in.

Each simulation case has been run for a maximum of 1825 days or roughly five years. The first five years usually represent the time period in which the recovery method can have the most influence on incremental and accelerated production. Some key indicators or points of influence include maximum oil production rate, plateau duration, rate of decline, timing of the injected phase breakthrough, and the impact on production ratios such as water cut and gas-to-oil ratio. Given the scale of sector models, results focus on the initial five-year period; however, extended duration cases were simulated and are briefly discussed.

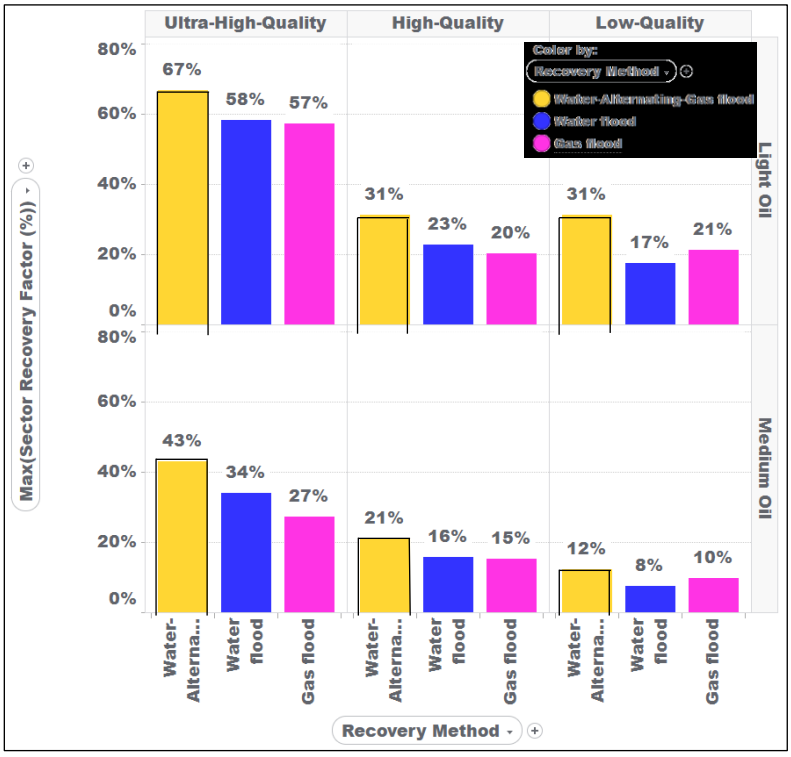

Figure 21: Results, Recovery Factor (%) by Simulation Case

The results in Figure 21 outline the final recovery factor for each of the simulations. It is observed that the WAG cases achieve the highest recovery in all six scenarios.

To begin the analysis, the case with highest recovery is considered the 'base case', and then the incremental recovery factor for the other two recovery methods is calculated in Table 5.

Recovery factor is calculated by dividing the cumulative oil produced (Sm^3) by the original oil in place or OOIP (Sm^3) for each sector model.

Table 5: Tabulated Recovery Factor differences for all Scenarios

Difference in Recovery Factor (%)									
Light Oil	**Ultra-High-Quality**			**High-Quality**			**Low-Quality**		
	WAG	**Water**	**Gas**	**WAG**	**Water**	**Gas**	**WAG**	**Water**	**Gas**
	Base	-9%	-10%	Base	-8%	-11%	Base	-14%	-10%
Medium Oil	**Ultra-High-Quality**			**High-Quality**			**Low-Quality**		
	WAG	**Water**	**Gas**	**WAG**	**Water**	**Gas**	**WAG**	**Water**	**Gas**
	Base	-9%	-16%	Base	-5%	-6%	Base	-4%	-2%

For the light oil cases, WAG yields a ~10% higher recovery factor for all three reservoir models, with the most improvement observed in the low-quality reservoir model when compared to the water flood case.

For medium oil, WAG yields the most improvement in the ultra-high-quality reservoir cases with a 9% incremental recovery factor gain over water flood. In the high-quality and low-quality reservoirs, this incremental recovery factor is lower, at 5% and 4% respectively.

Overall, these results align with the reviewed literature by Christensen et al. that suggested WAG increases recovery factor by 5% to 15% compared to water flood [3], [14], with a mean 10% increase in recovery factor using miscible WAG [14], which was also the case for these simulations.

This reviewed literature provides some validation of the results where a benefit to recovery is observed by implementing secondary WAG. Beyond this, it is difficult to further validate the results given the ongoing, confidential development planning for potential fields in the Flemish Pass and otherwise minimal public examples of secondary WAG projects on a global scale. Given this lack of analogous production history, further validation of WAG as a secondary recovery method is considered a future work scope.

4.1.1. Light Oil Cases

Before evaluating reservoir specific results, the charts in Figure 22 display recovery factor versus time for all of the light oil cases. These results allow one to draw further, coarse conclusions; however, evaluating phase breakthrough is best observed in Section's 4.2, 4.3, and 4.4.

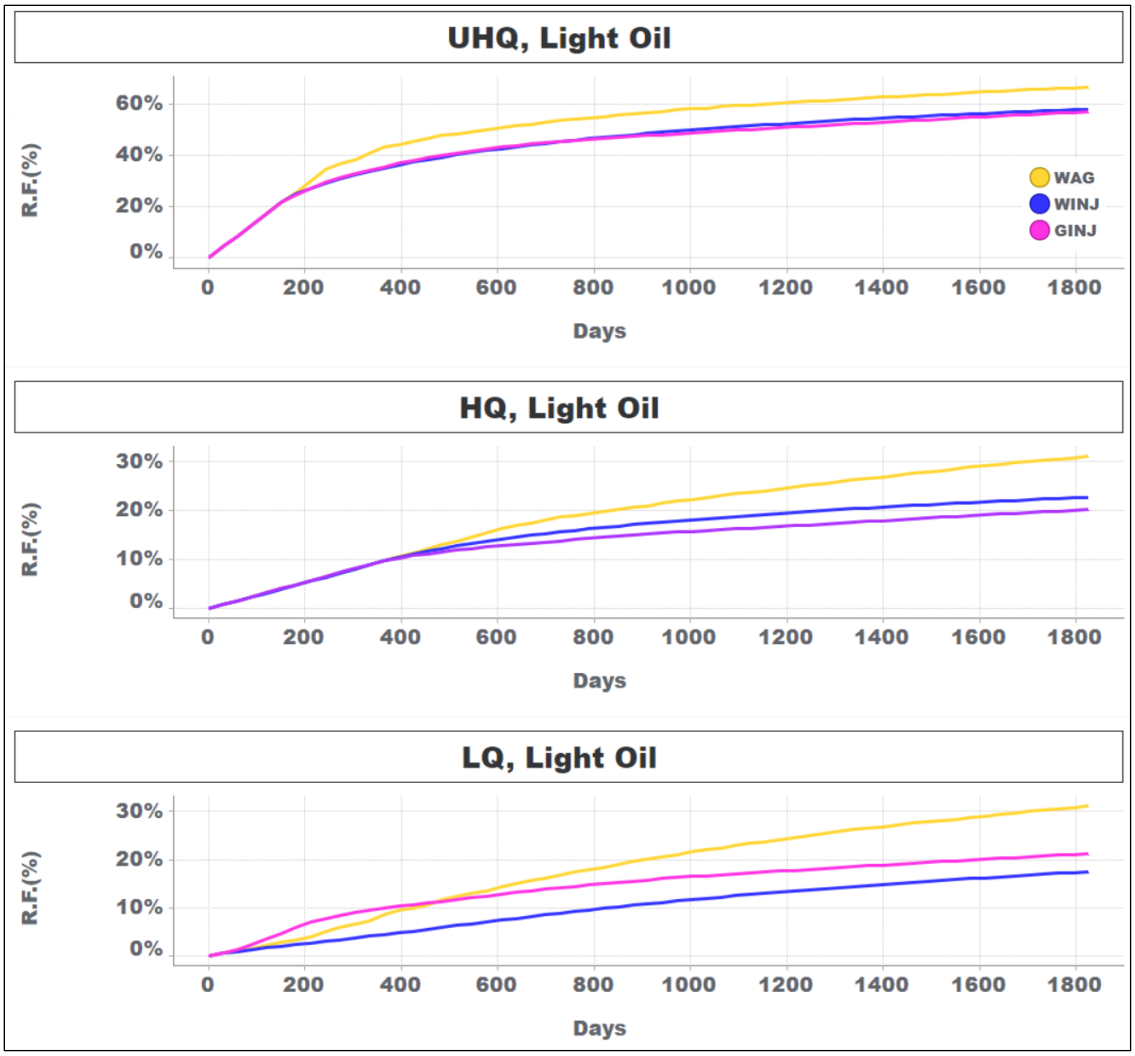

Figure 22: Recovery Factor charts for Light Oil cases

For the ultra-high-quality reservoir with light oil, observe the top chart in Figure 22 where all three recovery methods maintain identical profiles for the first 182 days or 6 months which indicates a production plateau. After this point, the WAG case diverges and continues along the same slope, maintaining the plateau, while the water flood and gas flood slopes decrease. This indicates a longer plateau for the WAG case which accelerates production and provides an incremental ~10% increase in recovery factor. There is minimal difference between the water and gas flood recovery factor profiles.

Moving on to the high-quality reservoir with light oil, observe the middle chart in Figure 22 where all three recovery methods maintain identical profiles during

production plateau for the first 400 days. This plateau is producing at a lower oil rate than the ultra-high-quality case; therefore, the plateau period is longer. After this point, the gas flood case declines the hardest, resulting in the lowest recovery factor curve, followed by the water flood case, and the WAG case. Notice that the recovery factor profile for the WAG case continues along a steeper slope compared to the other two recovery methods, for the entire duration of simulation.

Finally, for the low-quality reservoir with light oil, observe the bottom chart in Figure 22 where the three recovery methods diverge from the start. It is observed that the gas flood case maintains a short production plateau before beginning a steep decline. The water flood case appears to maintain consistent, yet non-plateau production for the entire duration of simulation, and the WAG case reaches a deferred production plateau once the production area is sufficiently pressure supported by the injection fluids.

4.1.2. Medium Oil Cases

Medium oil simulation results are displayed in Figure 23. Observe that all of the recovery factor profiles are more sporadic. Given that the medium oil has extremely low solution (dissolved) gas at reservoir conditions, this oil will have much lower fluid mobility. When you also account for the higher viscosity, roughly ~10x higher than the light oil, and higher density, it is obvious that the medium oil will have a more difficult time flowing, even from a high-pressured reservoir.

For the ultra-high-quality reservoir with medium oil, the gas flood case sees the steepest initial slope, while the WAG and water flood cases have mirrored profiles for the first ~120 days or 4 months. At this point, the WAG and water flood cases diverge as the WAG slope becomes steeper, indicating a more efficient sweep profile and better pressure support. The response indicates that the injection phase breakthrough with WAG is slightly delayed given the 2-month injection cycles and phase slugs.

Moving on to the high-quality reservoir which has reduced connectivity relative to the ultra-high-quality reservoir. Observe the slow, moderate slope to the recovery factor profiles for the initial 100 days. At this point, the gas flood case surges while the others continue along the same, initial slope. This appears to be a situation where the gas breakthrough correlates to an increase in well productivity. Once the WAG case begins to actively cycle gas and water from the injector well, the slope of the WAG profile increases substantially, ultimately resulting in the highest recovery factor at end of simulation.

Finally, the LQ reservoir has even further reduced connectivity, with a mean permeability of 166mD in sandstone. Observe another 120-day period of similar

profiles before the gas flood case surges. Once again, the slope of the WAG case will eventually increase once the producer is adequately pressure supported and the injection phases are actively cycling; however, it is not until late-time, around 3 years, that the WAG case recovery surpasses the gas flood recovery.

From these results, a common trend emerges. Injecting gas by means of gas flood and WAG flood result in a more uniform sweeping, miscible displacement process. In addition to the miscible conditions, gas flood and WAG flood also lower the viscosity of the producing fluid. These two concepts are observed during early time in the gas flood cases, and over the full span of production in the WAG flood cases. Overall, these characteristics result in a reservoir fluid with improved flow performance that is easier to produce and more economically viable to develop.

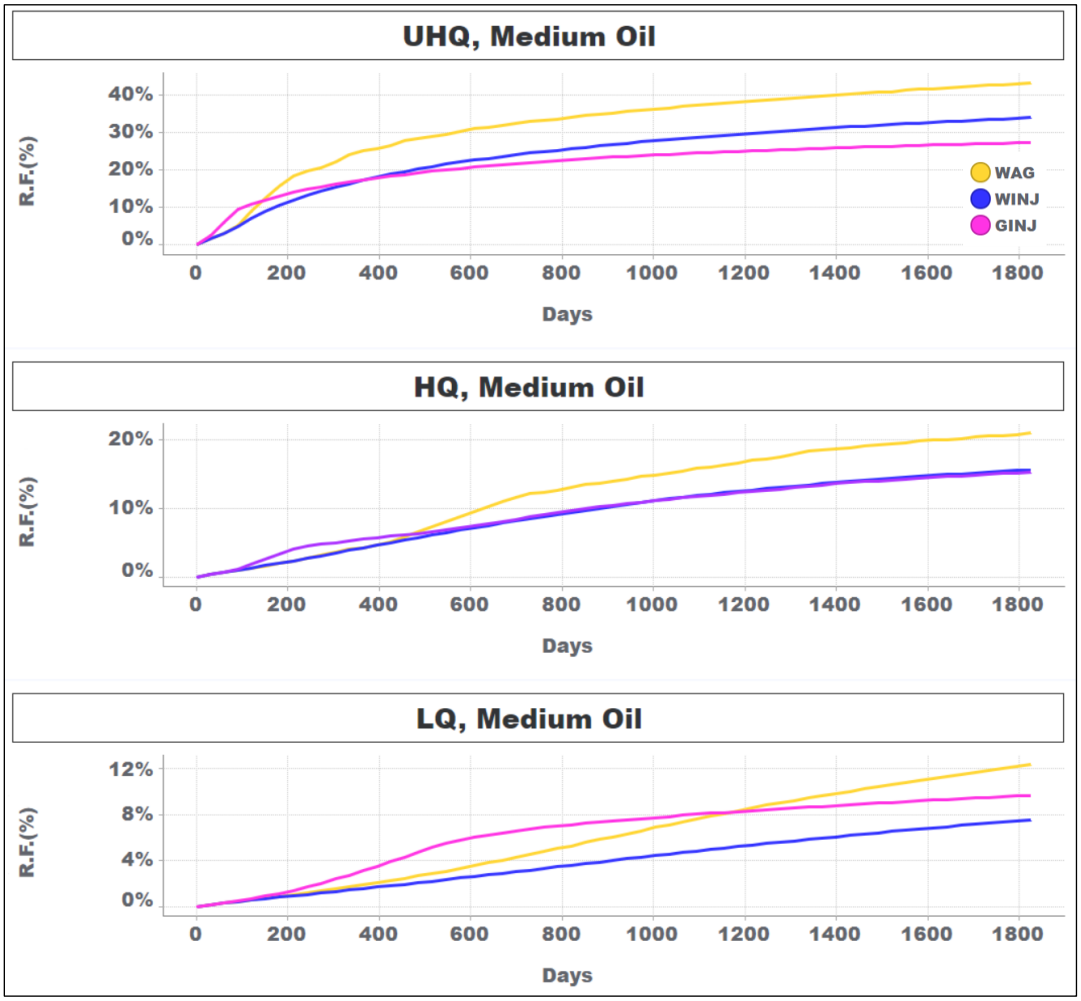

Figure 23: Recovery Factor charts for Medium Oil cases

4.1.3. Extended Duration Cases

As discussed in Development Strategies, some extended cases have been run for 20 years. These cases are used to evaluate the profile of recovery factor vs. pore volume injected, especially during late production life, and assess which recovery methods are most beneficial for the various reservoir and fluid models.

The line charts in Figure 24, Figure ***25***, and Figure 26 compare Recovery Factor and Pore Volume Injected. Results are shown for all water flood, gas flood, and water-alternating-gas flood simulation cases with a 20-year runtime.

Recovery factor is calculated and inherently normalized in relation to the Original Oil in Place (OOIP) for each specific sector model. This normalization allows recovery factor to be compared across the different quality reservoir models. As per the Development Strategies section, production constraints vary by reservoir model; therefore, it is not possible to compare the other simulation results on the basis of pore volume injected. Recovery factor is the only normalized parameter and therefore it is the only parameter compared in this manner.

Results from the extended cases are detailed below.

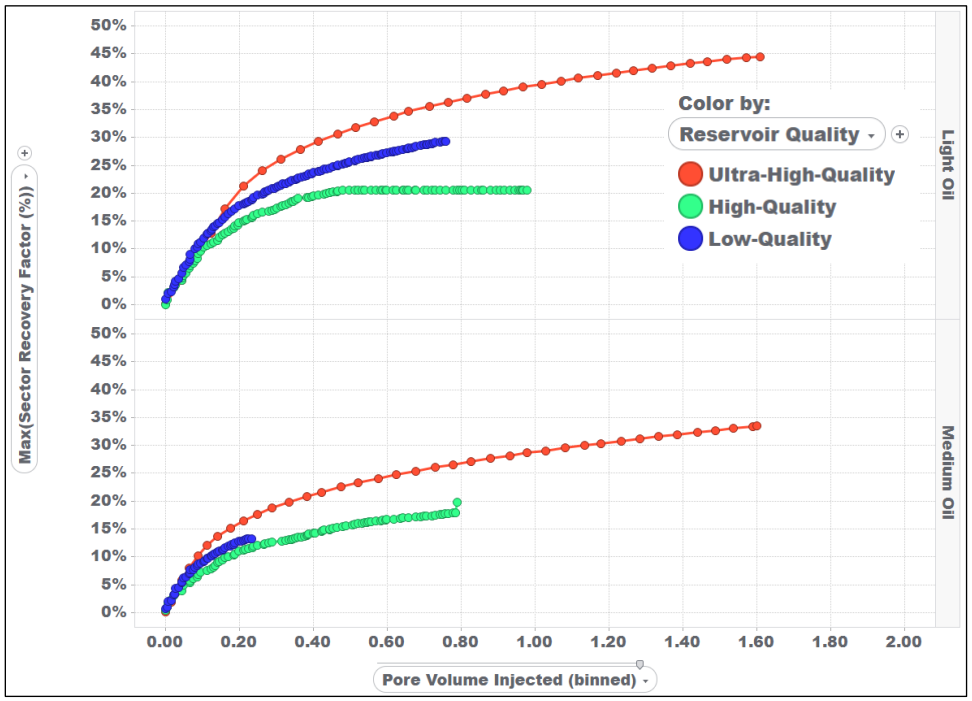

Figure 24: Extended Case 'Water flood' Results

The water flood results show a similar recovery profile for the light and medium fluid models, and water flooding appears successful for all three quality reservoirs.

The Ultra-High-Quality reservoir observes the best results from water flooding, followed by the Low-Quality then the High-Quality reservoir.

The Ultra-High-Quality is the last curve to deviate from the initial slope, meaning that water flood was able to maintain the production plateau longest in this reservoir. The initial high drainage rate can be attributed to the much higher mean horizontal permeability, 3,840 mD compared to 1,608 mD and 166 mD for the High and Low-Quality reservoir models. Also consider that the relative permeability curves have a broader region of mobile oil for the ultra-high-quality and high-quality reservoirs. This large primary drainage region combined with a very low connate water saturation and high mean permeability allow for high rate primary depletion and swift pressure support from the adjacent water injector. These characteristics result in high rate depletion for an extended plateau period.

For the initial 0.1 pore volume injected (PVI), all three water flood cases perform similarly. After 0.1 PVI, the Ultra-High-Quality reservoir continues on the same slope at its' production plateau rate. During the same period, the slope of the Low-Quality recovery is decreasing; however, the Low-Quality reservoir observes better recovery at less injected pore volume compared to the High-Quality reservoir. This is possible because of better sweep efficiency. Water flood is most efficient in continuous flow units of constant thickness with little heterogeneity, dip, or faulting.

Even though the Low-Quality reservoir has a slightly lower porosity and a much lower mean permeability, it is a constant thickness, continuous sand, with less dip and less faulting than the High-Quality sector model. These characteristics allow for a more efficient water flood sweep in the Low-Quality reservoir.

At 0.5 PVI, the high-quality water flood case shuts-in around 20% recovery factor due to reaching its bottom hole pressure limits and being unable to maintain productivity. At this point, the low-quality reservoir is still producing, having recovered ~25%, and the ultra-high-quality reservoir is at a ~32% recovery factor.

It is important to note that early shut-in's may be an artifact of simulation. In this case, the reservoir simulator may be shutting-in the production well prematurely if the sector model has too high productivity. Theoretically, the simulator should target the specified oil and liquid production rates while maintaining the specified minimum bottom hole pressure. If productivity is too high, the simulator may encounter issues converging on a solution and subsequently force a shut-in.

The results from light oil cases at end of production life are 45% recovery in the ultra-high-quality model, 30% in the low-quality model, and 20% in the high-quality

model. These results reaffirm favorable conditions for water flooding in well-connected reservoirs.

Results are similar with the medium oil cases; however, early shut-in times occur due to loss of well productivity while producing the ~dead oil. The three recovery profiles appear to be following the same general trends as the light oil cases.

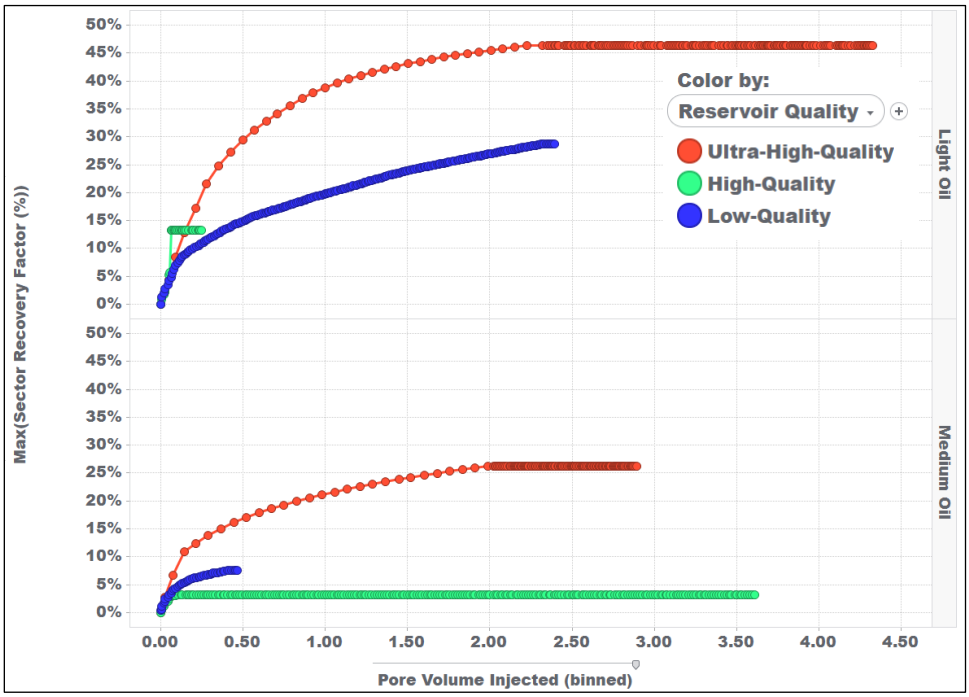

Figure** 25**: Extended Case 'Gas flood' Results

Moving on to the gas flood simulation cases outlined in Figure ***25*** above. The extended duration results are difficult to decipher due to early shut-in's and some sporadic data from the High-Quality reservoir model.

For the initial 0.1 pore volume injected, recovery from the High-Quality model follows a similar recovery profile to the others. In this case, gas flood on its own is not capable of supporting production in the High-Quality model given the added complexity from faulting, varying thickness, and heterogeneity. These reservoir characteristics lead to a high degree of gas fingering which subsequently leads to insufficient pressure support and causes sharp increases in produced gas that destabilize production and lead to a shut-in under the production constraints. This situation repeats for the medium oil fluid model simulation.

The recovery from the Low-Quality and Ultra-High-Quality models is more stable given the homogeneous, constant thickness sand packages in both sector models. Both gas flood cases follow the same profile for the initial 0.1 PVI; however, the

Low-Quality slope quickly decreases after 0.1 PVI due to the lack of adequate pressure support from gas injection. It appears that gas injection on its own is not sufficient in the Low-Quality model. This aligns with some literature findings that suggest the gas phase is partial to high permeability strata and will sometimes bypass relatively low permeability zones [3], [4]. As a result, the gas phase may be channeling in the Low-Quality reservoir and not providing an efficient sweep. The Low-Quality models observes a gradual yet constant increase in recovery factor as PVI continues to increase. The light oil simulation shut's in due to production constraints around 2.25 PVI with a recovery factor of ~28%.

Finally, in the Ultra-High-Quality model, the initial recovery slope is constant for roughly 0.25 PVI with light oil and 0.15 PVI with medium oil. After this production plateau ends, the recovery slope decreases at an even more gradual rate compared to the other reservoir models. This gradual decrease in recovery slope indicates stable pressure support and reservoir depletion with the gas flood recovery. At 2.25 PVI, the Ultra-High-Quality model has a final recovery factor around ~45%. This high recovery factor indicates that gas flood is a valid option for a reservoir of these highest quality characteristics where there are minimal flow impedances that could lead to gas fingering or channeling.

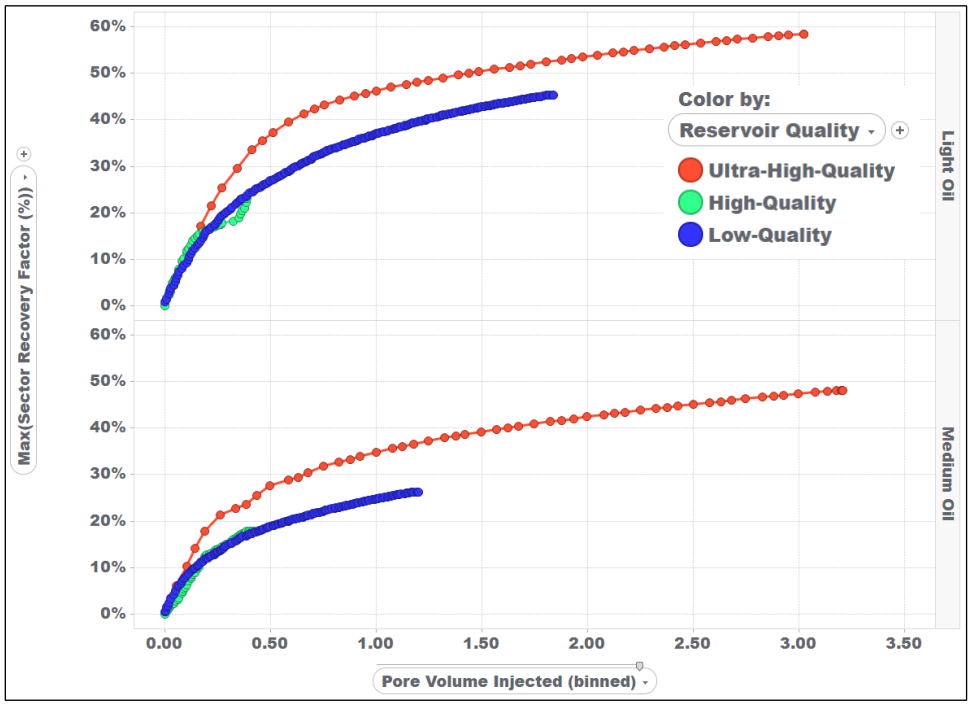

Figure 26: Extended Case 'WAG flood' Results

The water-alternating-gas flood cases shown in Figure 26 produce the most consistent results over extended durations. All of the cases maintain some form of long-term production with similarly shaped recovery profiles.

As observed above, the Low-Quality and High-Quality reservoir results are virtually identical, with 0.5 PVI recovery factors of ~27% for light oil cases and ~20% for medium oil cases. This is significantly higher recovery than observed with the water flood and gas flood scenarios. At the end of production life, the Low-Quality and High-Quality reservoir achieve a ~45% recovery factor at 1.8 PVI for light oil and a ~25% recovery factor at 1.25 PVI for medium oil.

The benefit of WAG appears to be relatively consistent across the Low and High-Quality models; however, the most benefit is observed in the Ultra-High-Quality reservoir where extended production life results in upwards of a 60% recovery factor with light oil and a 50% recovery factor with medium oil, at 3.0 pore volumes injected. The slope of the recovery profile gradually declines after the initial ~0.25 pore volumes injected; however, recovery continues to increase as the two-phase injection is continuously cycled and in-turn provide a consistent level of pressure support and reservoir sweep.

4.1.4. Hysteresis

During the setup stage of simulation, hysteresis was tested on the ultra-high-quality reservoir WAG case. The test case used Killough's hysteresis model for the non-wetting phases and used the drainage curve from the wetting phase. This test case produced very similar results to the case without a hysteresis model. Results were similar in terms of pressure response and production/injection rates; however, after the initial production plateau period, the case with hysteresis enabled observed slightly different phase behaviour that resulted in a lower GOR, more fluctuating water cut, and overall +7% higher cumulative oil production after 5 years. Due to increased run-time, it was determined that implementing hysteresis for all eighteen simulation cases was not feasible. Given that the results of this study will be evaluated relative to one another, potential over or underestimation of produced oil and gas volumes, due to the lack of a hysteresis model, should not have any impact on the basis of conclusions. Results are located in Appendix A.

4.2. Ultra-High-Quality (UHQ) Reservoir Results

The ultra-high-quality reservoir sector model has a mean sandstone permeability of 3.8 Darcy, mean porosity of 25.2% with a truncated, relatively uniform thickness of 20m. This reservoir is modelled to reflect results of conventional core and well log data extracted from exploration wells in the Flemish Pass. This example of ultra-high-quality reservoir is uncommon in most producing Jeanne d'Arc Basin assets, making this an appealing frontier for potential development. Given the high level of geological quality and high reservoir pressures, the results from sector model simulation indicate an ease of producing from this reservoir while encountering some difficulties in restricting the produced Gas-to-Oil Ratio and Water Cut.

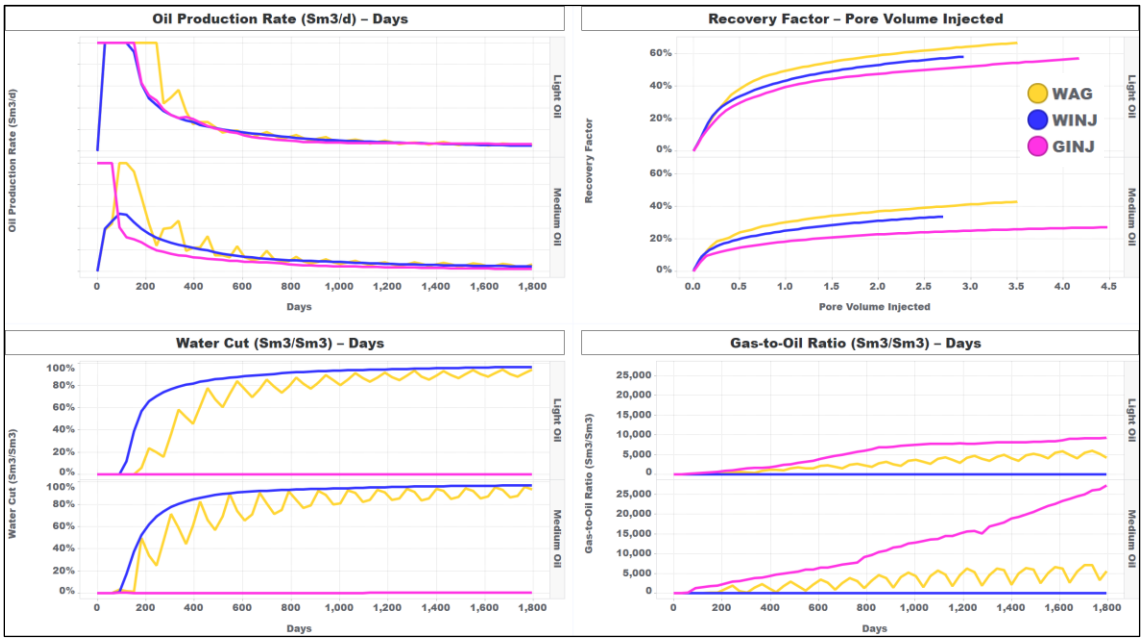

Figure 27: Results for UHQ, Light and Medium Oil cases

The ultra-high-quality results indicate that WAG significantly improves recovery for both light and medium oil cases.

For light oil cases, WAG extends the production plateau relative to gas flood and water flood cases while also delaying water and gas breakthrough, as observed from the water cut and GOR charts. This delay can be attributed to the alternating cycles of water and gas injection which allows pressure support to build while reducing slugging of a single phase between the injector and producer. Observe

from Table 6 that recovery factor at equivalent PVI's is much higher with WAG than water flood or gas flood.

Table 6: Tabulated Recovery Factor by PVI Increments (UHQ, Light Oil)

Pore Volume Injected	WAG RF (%)	WINJ RF (%)	GINJ RF (%)
0.5	39	34	30
1.0	49	44	39
1.5	55	49	45
2.0	59	53	48
2.5	62	56	50

The ultra-high-quality reservoir with medium oil cases illustrate a delayed plateau with WAG. In the WAG case, injection begins with water before switching to gas injection after 2 months. The varying water-cut and gas-to-oil ratio profiles for the WAG case can be attributed to these injection cycles. Results indicate that once the injected gas reaches the producer, it acts to reduce the viscosity and increase the mobility of the medium oil. At this point, the oil is able to flow at a higher rate and reaches production plateau, maintaining the plateau rate for approximately 30 days before the rate declines. Observe a similarly delayed water and gas breakthrough compared to the single-phase injection cases.

It is observed from Table 7 that the WAG case is able to achieve a higher recovery factor at each of the incremental PVI's; however, there is less spread in recovery factor at low PVI's (PVI < 0.25) after which point the three curves begin to diverge.

Table 7: Tabulated Recovery Factor by PVI Increments (UHQ, Medium Oil)

Pore Volume Injected	WAG RF (%)	WINJ RF (%)	GINJ RF (%)
0.5	24	20	15
1.0	30	25	18
1.5	34	28	21
2.0	37	31	23
2.5	39	33	24

In summary, the ultra-high-quality cases indicate that WAG is a suitable option for both light and medium oil cases.

For the light oil cases, WAG extended the production plateau, delayed injection phase breakthrough, allowed the water cut to remain 5% to 10% below the water flood case during mid-to-late life, and positively influences recovery factor at PVI > 0.3.

For the medium oil cases, gas flood was the most impactful injection phase as it adds much needed energy to the nearly dead oil; however, injecting only gas causes the produced GOR to increase substantially during mid-to-late life. WAG provides a good balance in providing pressure support without significant water or gas production. This is observed from the drastically different gas-to-oil ratio profiles in Figure 27.

The gas flood case with medium oil results in a much higher produced GOR, around 27,000 Sm3/Sm3 at the final timestep, as the system requires gas to improve the well productivity. This can be compared to roughly 9,000 Sm3/Sm3 at the final timestep for the light oil case.

Similarly, WAG with medium oil results in a produced GOR fluctuating around 5,000 Sm3/Sm3 at the final timestep with large amplitude oscillations, compared to the light oil case that also fluctuates around 5,000 Sm3/Sm3 with smaller amplitude oscillations.

The water cut profiles are very similar between the light and medium oil cases given that water-oil interaction is relatively similar regardless of the oil density. With that said, the difference in viscosity between the two oils does lead to a higher water flood recovery factor with the light oil. At comparable pore volumes injected, the light oil case recovery factor is 15% to 23% higher than the medium oil case when undergoing water flooding.

4.3. High-Quality (HQ) Reservoir Results

The high-quality reservoir sector model has a mean sandstone permeability of 1.6 Darcy and a mean sandstone porosity of 21.6%, which can be considered analogous, purely in terms of these parameters, to some producing fields in the Jeanne d'Arc Basin. The sector model has a varying reservoir thickness of 5 to 15m. The challenge associated with these high-quality simulation cases involves maintaining a lower rate, longer duration production plateau while staying above the bottom hole pressure limit and allowing for consistent productivity.

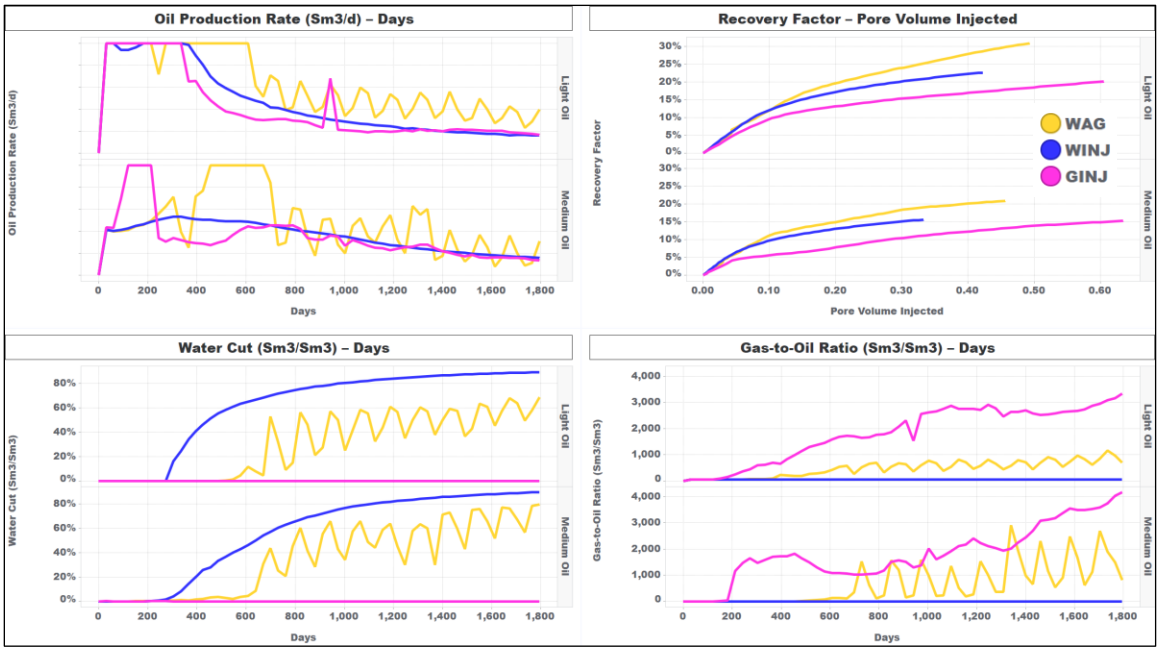

Figure 28: Results for HQ, Light and Medium Oil cases

The high-quality results indicate similar findings to the ultra-high-quality results.

In the light oil cases, WAG successfully extends the production plateau for nearly double the duration of the single-phase injection cases. WAG achieves this feat while delaying the water cut onset significantly, maintaining a lower water cut, albeit oscillating, than the water flood case, and achieving higher recovery factor with less injected volume than the gas flood case. This is outlined by the tabulated PVI data below.

Table 8: Tabulated Recovery Factor by PVI Increments (HQ, Light Oil)

Pore Volume Injected	WAG RF (%)	WINJ RF (%)	GINJ RF (%)
0.1	12	12	10
0.2	20	17	13
0.3	24	20	15
0.4	28	22	17

For the medium oil cases, it is difficult to maintain stable production. The gas flood case eventually reaches a short production plateau for ~3 months while the water flood case never does reach plateau. The combination of water and gas injection eventually helps the WAG case reach a production plateau after 15 months on production, for a plateau period of 7 months.

This difficulty in maintaining stable production is reiterated in the GOR plot where the sporadic nature of the gas flood case results are observed from the initial rapid onset of gas around the 200-day mark. The GOR then remains relatively constant before temporarily declining and then climbing again at the 800-day mark.

Table 9: Tabulated Recovery Factor by PVI Increments (HQ, Medium Oil)

Pore Volume Injected	WAG RF (%)	WINJ RF (%)	GINJ RF (%)
0.1	11	10	6
0.2	15	13	8
0.3	18	15	11

The recovery factor spread at the PVI increments above is significantly less than observed from the light oil cases. There is minimal difference between the water flood and WAG recovery factor until you reach beyond 0.2 PVI, at which time the gas volumes injected with the WAG case allow the recovery factor profile to increase at a steeper slope compared to the water flood case.

This result reinforces the positive impact of injecting gas into the nearly dead, medium oil. It also becomes clearer that the gas injection WAG cycle could be better optimized for this reservoir. A simple optimization would be to inject more gas upfront in order to reach production plateau sooner, similar to the gas flood case, and then transition to a more equally weighed gas and water injection cycle. This would provide better acceleration while still yielding the incremental recovery factor as shown in the PVI chart.

4.4. Low-Quality (LQ) Reservoir Results

The low-quality reservoir sector model has a mean sandstone permeability of 166 millidarcy and a mean sandstone porosity of 20.6%, which can be considered analogous, purely in terms of these parameters, to several producing fields in the Jeanne d'Arc Basin. This sector model has a relatively constant reservoir thickness of 20m. Generally, wells in this quality reservoir can produce for a longer period of time at low rates before reaching the water cut or gas-to-oil ratio shut-in limits. This is the opposite of the ultra-high-quality model where one of the difficulties is providing enough injection support to maintain a high rate plateau while limiting water and gas breakthrough due to the ultra-high permeability.

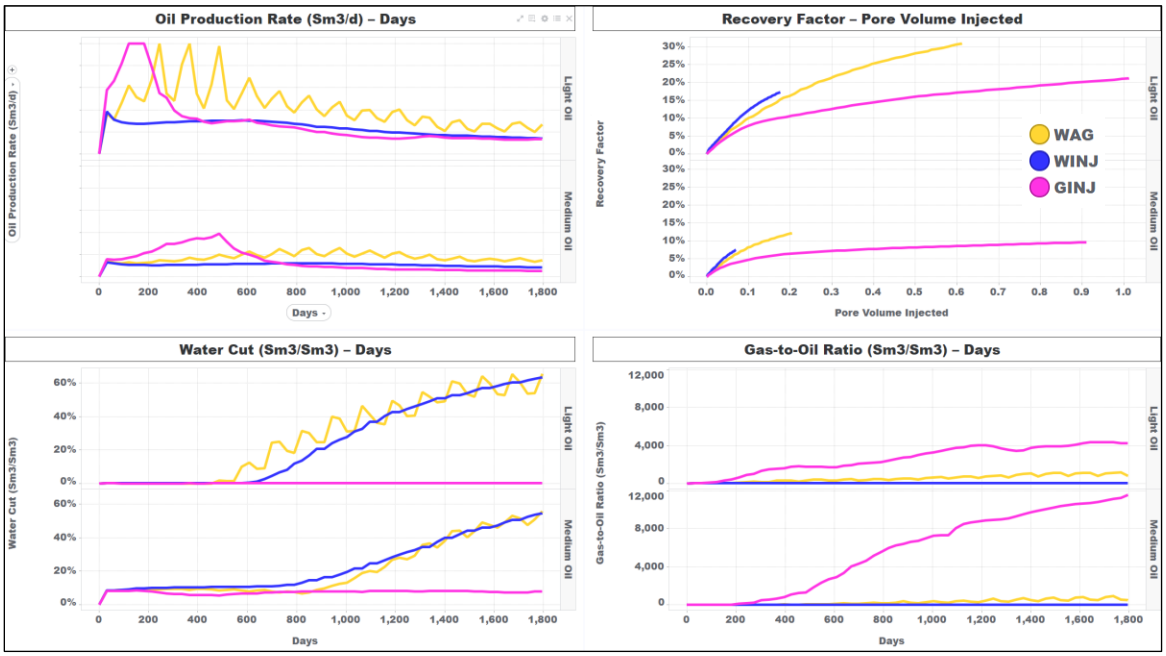

Figure 29: Results for LQ, Light and Medium Oil cases

In the light oil cases, the gas flood case achieves a brief production plateau, the water flood case does not reach plateau, and the WAG case mirrors the water flood case during its initial water injection cycle, eventually improving due to gas cycle support. The WAG case does not reach plateau; however, it does maintain a higher rate than the single-phase injection cases, oscillating heavily depending on which phase is being injected. Water breakthrough is relatively similar between the WAG and water flood cases, with the WAG case observing breakthrough first, perhaps due to phase mixing. Gas breakthrough is also similar, with the gas flood case eventually reaching a GOR around 4,000 Sm3/Sm3 and the WAG case reaching 1,100 Sm3/Sm3.

The medium oil cases are unstable and likely uneconomic due to the cost to develop and produce in a deep-water offshore environment. With very low production rates, the only potential recovery method may be single-phase gas flood recovery method, after significant optimization.

Given the improved production, lower GOR, and similar water cut profile, it is clear that this low-quality reservoir receives the most benefit from utilizing WAG, compared to the high-quality and ultra-high-quality reservoirs. It is difficult to compare PVI for these cases as the PVI is very low due to the relatively small volumes produced, and in-turn small volumes needed for pressure support.

4.5. WAG Secondary vs. Tertiary (EOR) Recovery Methods

Water-alternating-gas injection has historically been used as an enhanced oil recovery (EOR) – or tertiary – recovery method [14]. The primary intent of this study is to evaluate WAG as a secondary recovery method alongside water flooding and gas flooding. On its own, this intent does not quantify how beneficial secondary WAG is compared to tertiary WAG. In attempt to capture this difference, six additional simulation cases – one in each reservoir and fluid model – were run to compare recovery of secondary versus tertiary WAG. The six cases utilize water flooding until they reach 80% water cut, at which point the injector switches to WAG using the same parameters as the secondary WAG cases.

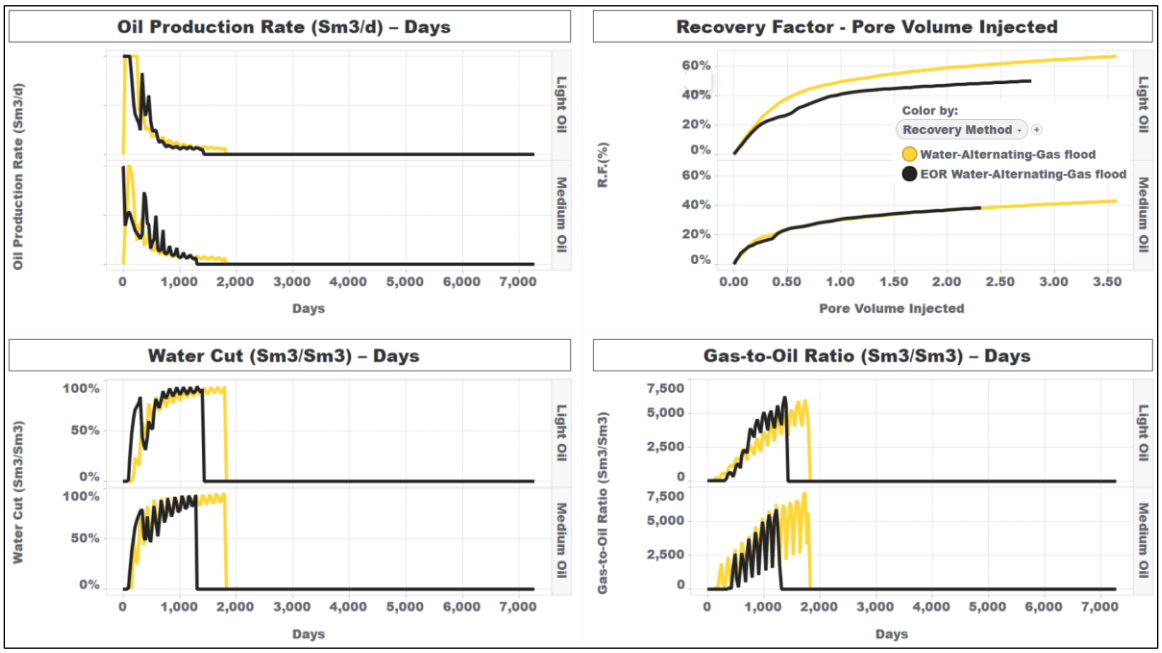

Figure 30: UHQ Reservoir, WAG, Secondary vs. EOR Recovery Method

Using tertiary or EOR WAG results in an incremental increase in recovery factor over water flooding. With that said, the hypothesis is that secondary WAG should still result in higher recovery than tertiary WAG given the longer duration of alternating phase injection, higher sustained sweep efficiency, and lower water cut.

Observe in Figure 30, Figure 31, and Figure 32 that at the same pore volume injected (PVI) ratio, secondary WAG tends to achieve more recovery than tertiary WAG in both the Ultra-high and High-quality light oil cases. In the Low-quality reservoir, secondary WAG has a much higher oil production rate for the initial five-year production period which yields significant production acceleration. For medium oil cases, tertiary and secondary WAG ultimately achieve similar recovery; however, the secondary WAG case has higher initial production rates.

Secondary WAG is more beneficial for light oils in all three different quality reservoirs. For medium oils, there is less of a delta between the recovery factors; however, production acceleration and lower water cut also promote secondary WAG as the better option.

As observed from the Ultra-high-quality and High-quality results, water breakthrough is delayed considerably with secondary WAG compared to water flood with tertiary WAG. This delayed breakthrough allows secondary WAG to yield a longer production life before shutting in due to water cut constraints. Consider the 'Recovery Factor – Pore Volume Injected' chart in Figure 31 below. The results demonstrate how the tertiary implementation of WAG has a positive impact and causes a step change in the trajectory of the recovery factor profile. This is even more pronounced in the medium oil case where the recovery from tertiary WAG eventually achieves the same as secondary WAG. Tertiary WAG also does well in the light oil case as it extends the overall production period and increases recovery over water flooding; however, tertiary WAG does not achieve the same recovery as secondary WAG. In this scenario, tertiary WAG is a lost opportunity to effectively sweep the reservoir and accelerate oil production.

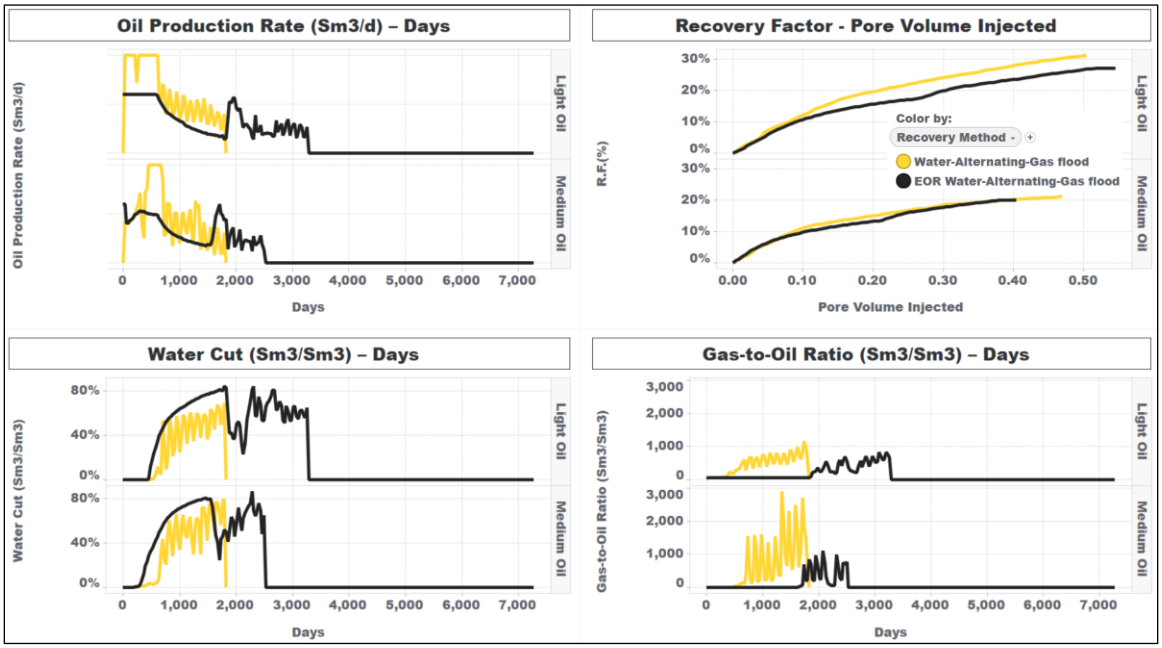

Figure 31: HQ Reservoir, WAG, Secondary vs. EOR Recovery Method

Next, recall from the original Low-quality model results (Figure 29) that the WAG and water flooding cases did best in maintaining pressure support given that the Low-quality reservoir benefits greatly from water flooding.

Keeping this in mind, it makes sense that when tertiary EOR is activated in the medium oil case, post water flood, the production well shuts in due to lack of pressure support shortly after gas phase injection is initiated. The low-quality reservoir does not respond well to gas sweep.

For the low quality, light oil case, tertiary WAG provides sufficient pressure support and the result is an immediately increased oil rate and decreased water cut. These characteristics allow the light oil case to produce for an additional ~10 years while maintaining stable production at a water cut around 80%.

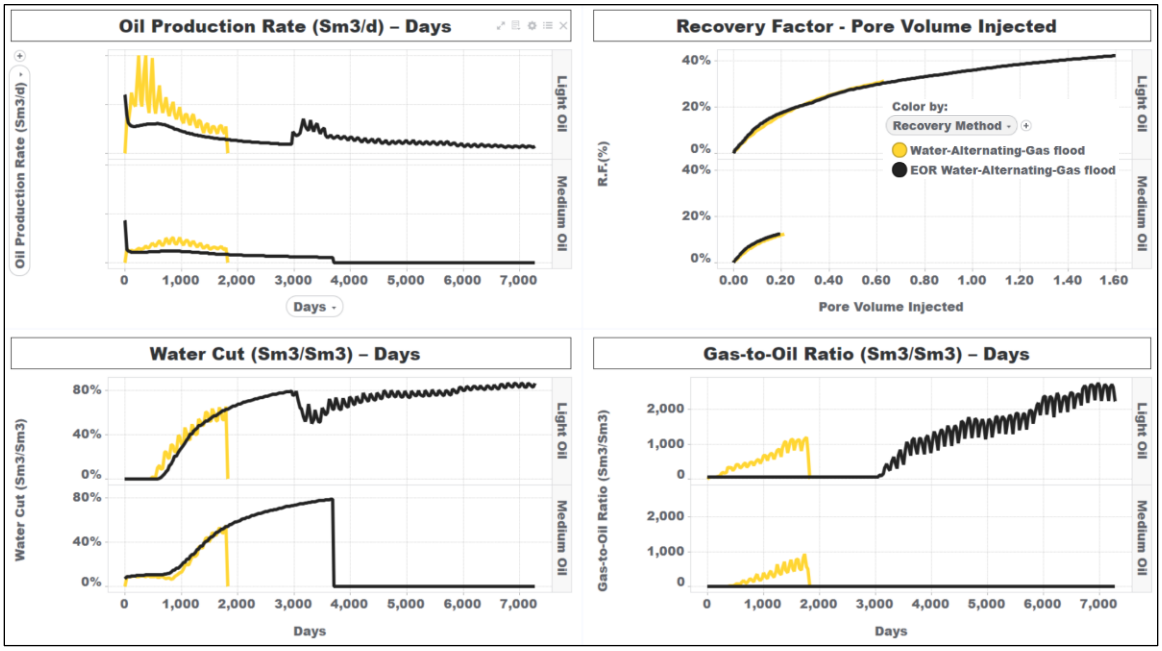

Figure 32: LQ Reservoir, WAG, Secondary vs. EOR Recovery Method

Overall, implementing WAG as a secondary recovery method has several benefits over WAG as an EOR or tertiary recovery method. In all of the cases, secondary WAG results in a higher initial oil production rate while simultaneously achieving the same or higher recovery factor at each PVI or 'pore volume injected' interval. This equates to accelerated and incremental oil production, and higher sweep efficiency per PVI for secondary WAG.

In some cases, tertiary WAG is able to achieve the same ultimate recovery factor as secondary WAG; however, this is uncertain and generally requires a much longer production life, therefore missing out on the accelerated oil production. Further to these benefits, secondary WAG also lessens facility burden associated with excess gas handling. For example, the detrimental environmental impacts of gas flaring and the added capital expenditure required to drill and complete gas disposal wells, can be largely avoided by using produced gas for secondary WAG.

5. Conclusions and Recommendations

5.1. Conclusions

5.1.1. General Notes

- With Light Oil, WAG yields a ~10% increase in recovery factor over both water flood and gas flood, with the most benefit observed in the ultra-high-quality reservoir. WAG may extend the production plateau by as much as 60% to 80% depending on the reservoir quality and production constraints.
- With Medium Oil, WAG yields a 4% to 9% increase in recovery factor over water flood, and a 2% to 16% increase in recovery factor over gas flood, with the most benefit observed in the ultra-high-quality reservoir. The production plateau periods with WAG are deferred but similar in duration.
- Simulation results indicate that WAG is a suitable option for both light and medium oils. High produced GOR may be flagged as a risk if the gas-to-oil injection ratio is high. This risk can be offset with the implementation of artificial lift solutions such as downhole gas lift or a subsea pump while maintaining a more equal, gas-to-water injection ratio.
- WAG Hysteresis does affect phase behaviour and testing resulted in +7% higher cumulative oil production after 5 years with hysteresis enabled.
- Water flood does best in low quality, highly connected reservoirs with continuous, homogeneous sands. Water flood for light oil cases achieve ~30% recovery factor in low-quality reservoir and ~45% recovery factor ultra-high-quality reservoir. Recovery factor for medium oil cases range from 13% to 34% depending on quality.
- Gas flood is more applicable for less connected reservoirs than water flood; however, the tendency of gas flooding to target higher permeability strata [3] can lead to gas channeling or fingering which can result in instable production and inefficient reservoir sweep. Gas flood for light oil cases achieve a ~28% recovery factor in low-quality reservoir and a ~45% recovery factor in ultra-high-quality reservoir. Gas flood recovery with medium oil is difficult to predict due to the early shut-in's; however, cases averaged a ~20% lower recovery factor than the light oil equivalent. Optimization of a gas flood depletion plan would likely improve this recovery for both fluid models.
- Water-alternating-gas (WAG) flood is observed to be beneficial for all reservoirs, even the more heterogenous high-quality reservoir. Alternating phases allow for a more balanced reservoir sweep and improved pressure support. Recovery factors for light oil cases range from 45% in low-quality and high-quality reservoir, to 60% in the ultra-high-quality reservoir.

Recovery factors for medium oil cases range from 25% in low-quality and high-quality reservoirs, to 50% in the ultra-high-quality reservoir.

- WAG, Secondary vs. Tertiary (EOR) recovery methods: Secondary WAG is more beneficial for light oil reservoirs in all three different quality models. Secondary WAG yields a higher ultimate recovery factor with the additional benefits of accelerated oil production, improved sweep efficiency, reduced facility burdens, and lower water cut than tertiary WAG. Secondary WAG is less beneficial for medium oil reservoirs as tertiary WAG eventually reaches a similar recovery factor; however, production acceleration and lower water cut are still observed with secondary WAG in medium oil reservoirs.
- Tertiary (EOR) WAG is most beneficial in low to medium-quality reservoirs where, once initiated, results in an immediate increase in oil rate and decrease in water cut, allowing for extended, stable production. In low to medium-quality reservoirs, tertiary and secondary WAG ultimately achieve the same recovery factor. Secondary WAG brings the benefit of production acceleration while tertiary WAG brings extended duration production which may be more beneficial in some cases.
- Tertiary (EOR) WAG simulations resulted in a consistent ~4% increase in recovery factor over the base water flood cases.

5.1.2. Comparison of WAG to Water flooding

- In the ultra-high-quality reservoir, water breakthrough with WAG occurs after 5 months (2.5 injection slugs) or 0.2 PVI, compared to breakthrough during water flood that occurs after 3 months or 0.1 PVI.
- WAG delays water breakthrough by 66% (UHQ) and 34% to 78% (HQ). WAG does not delay water breakthrough in the low-quality reservoir. Water breakthrough occurs faster in lower quality reservoir and is more delayed in higher quality reservoir. This can be attributed to the water phase preferentially sweeping lower quality reservoir.

5.1.3. Comparison of WAG to Gas flooding

- In the ultra-high-quality reservoir, gas breakthrough with WAG occurs after 6 months (3.0 injection slugs) or 0.3 PVI, compared to breakthrough during gas flood that occurs after 2 months or 0.1 PVI.
- WAG delays gas breakthrough by 100% (UHQ), 145% to 220% (HQ), and 170% to 250% (LQ). Gas breakthrough occurs faster in higher quality reservoir and is more delayed in lower quality reservoir. This can be attributed to the gas phase preferentially sweeping higher quality reservoir.

5.2. Recommendations

Listed below are recommendations for continuing research into the topics discussed within this study. These recommendations may act as next steps in further evaluating conclusions from Section 5.1 with added focus on a variety of topics. Topics may include further evaluation of WAG as a secondary recovery method, simulating hysteresis with compositional fluid models, and optimization of WAG design parameters, manually or using machine learning.

Specific recommendations for future work:

- Modify production constraints to extend simulation duration and improve injectivity with the goal of attaining higher Pore Volume Injected (PVI) ratios for improved definition of PVI profiles for each quality reservoir.
- Run all simulations with hysteresis enabled to evaluate the sensitivity of each model to the hysteresis process, and the subsequent impact on dynamic model output parameters; such as, water cut, gas-to-oil ratio, production rates, and pressure response.
- Optimize WAG schemes by evaluating dynamic model outputs and adjusting the WAG input parameters; such as, duration of gas and water injection cycles, injection rates, and cycle ratios. This iterative process could be further optimized using machine learning techniques to evaluate simulation results and automatically adjust the input parameters.
- Evaluate the impact of learnings from this study by conducting full field simulations for applicable implementation candidates.

6. References

[1] Schlumberger, “ECLIPSE Compositional Simulator,” 2020. https://www.software.slb.com/products/eclipse/simulators/compositional-simulator.

[2] V. Vishnyakov, B. Suleimanov, A. Salmanov, and E. Zeynalov, “7 - Oil recovery stages and methods,” V. Vishnyakov, B. Suleimanov, A. Salmanov, and E. B. T.-P. on E. O. R. Zeynalov, Eds. Gulf Professional Publishing, 2020, pp. 53–63.

[3] S. Afzali, N. Rezaei, and S. Zendehboudi, “A comprehensive review on Enhanced Oil Recovery by Water Alternating Gas (WAG) injection,” *Fuel*, vol. 227, pp. 218–246, 2018, doi: https://doi.org/10.1016/j.fuel.2018.04.015.

[4] K. S. Sorbie, R. M. S. Wat, and T. C. Rowe, “Oil displacement experiments in heterogeneous cores: analysis of recovery mechanisms,” 1987.

[5] Corporatefinanceinstitute.com, “Straight Line Depreciation,” 2020. https://corporatefinanceinstitute.com/resources/knowledge/accounting/straight-line-depreciation/ (accessed Nov. 18, 2020).

[6] D. Piper and D. Campbell, “Quaternary geology of Flemish Pass and its application to geohazard evaluation for hydrocarbon development,” *Pet. Resour. Reserv. Gd. Banks, East. Can. margin*, vol. 43, p. 29, Jan. 2005.

[7] C-NLOPB, “Schedule of Wells,” *Canadian Petroleum*, 2020. https://www.cnlopb.ca/wells/ (accessed Nov. 08, 2020).

[8] C-NLOPB, “Land Registry System,” 2020. https://www.cnlopb.ca/abstract/#list.

[9] T. Roberts, “Equinor inching closer to sanctioning ‘world class’ Bay du Nord field,” *CBC NL*, St. John’s, NL, Oct. 10, 2019.

[10] Equinor ASA, “Bay du Nord (BdN) Project Location,” 2020. https://www.equinor.com/en/where-we-are/canada-bay-du-nord.html (accessed Nov. 17, 2020).

[11] E. D. Haugen, J. P. Costello, L. B. Wilcox, E. Albrechtsons, and I. Kelly, “Reservoir Management Challenges of the Terra Nova Offshore Field: Lessons Learned After 5 Years of Production,” *SPE Annual Technical Conference and Exhibition*. Society of Petroleum Engineers, Anaheim, California, U.S.A., p. 15, 2007, doi: 10.2118/109587-MS.

[12] B. Al Shehhi, H. Patel, Z. Jani, and S. Khan, “Implementation Study for Miscible Water Alternating Gas (WAG) EOR in a Giant, Offshore Field,” *SPE Middle East Oil & Gas Show and Conference*. Society of Petroleum

Engineers, Manama, Bahrain, p. 11, 2015, doi: 10.2118/172787-MS.

[13] K. P. Ramachandran, O. N. Gyani, and S. Sur, “Immiscible Hydrocarbon WAG: Laboratory to Field,” *SPE Oil and Gas India Conference and Exhibition*. Society of Petroleum Engineers, Mumbai, India, p. 11, 2010, doi: 10.2118/128848-MS.

[14] J. R. Christensen, E. H. Stenby, and A. Skauge, “Review of WAG Field Experience,” *SPE Reserv. Eval. Eng.*, vol. 4, no. 02, pp. 97–106, 2001, doi: 10.2118/71203-PA.

[15] J. R. Christensen, E. H. Stenby, and A. Skauge, “Compositional and Relative Permeability Hysteresis Effects on Near-Miscible WAG,” *SPE/DOE Improved Oil Recovery Symposium*. Society of Petroleum Engineers, Tulsa, Oklahoma, p. 16, 1998, doi: 10.2118/39627-ms.

[16] E. Britannica, “Wet gas,” *The Editors of Encyclopaedia Britannica*. https://www.britannica.com/science/wet-gas (accessed Nov. 20, 2020).

[17] A. L. Bunge and C. J. Radke, “CO2 Flooding Strategy in a Communicating Layered Reservoir,” *J. Pet. Technol.*, vol. 34, no. 12, pp. 2746–2756, 1982, doi: 10.2118/10289-PA.

[18] D. J. Element, J. H. K. Masters, N. C. Sargent, A. J. Jayasekera, and S. G. Goodyear, “Assessment of Three-Phase Relative Permeability Models Using Laboratory Hysteresis Data,” *SPE International Improved Oil Recovery Conference in Asia Pacific*. Society of Petroleum Engineers, Kuala Lumpur, Malaysia, p. 11, 2003, doi: 10.2118/84903-MS.

[19] E. T. S. Huang and L. W. Holm, “Effect of WAG Injection and Rock Wettability on Oil Recovery During CO2 Flooding,” *SPE Reserv. Eng.*, vol. 3, no. 01, pp. 119–129, 1988, doi: 10.2118/15491-PA.

[20] J. P. Srivastava, “Water alternating gas (WAG) injection a novel EOR technique for mature light oil fields a laboratory investigation for GS-5C sand of gandhar field,” 2012.

[21] M. M. Kulkarni and D. N. Rao, “Experimental Investigation of Various Methods of Tertiary Gas Injection,” *SPE Annual Technical Conference and Exhibition*. Society of Petroleum Engineers, Houston, Texas, p. 11, 2004, doi: 10.2118/90589-MS.

[22] M. M. Kulkarni and D. N. Rao, “Experimental Investigation of Miscible Secondary Gas Injection,” *SPE Annual Technical Conference and Exhibition*. Society of Petroleum Engineers, Dallas, Texas, p. 8, 2005, doi: 10.2118/95975-MS.

[23] L. Belazreg, S. M. Mahmood, and A. Aulia, “Novel approach for predicting

water alternating gas injection recovery factor," *J. Pet. Explor. Prod. Technol.*, vol. 9, no. 4, pp. 2893–2910, 2019, doi: 10.1007/s13202-019-0673-2.

[24] R. H. Mohammad Kowsari, Lesley James, "The Effect of Relative Permeability Hysteresis on the Design of an Optimal Water-Alternating-Gas (WAG) Process," Memorial University of Newfoundland, 2020.

[25] A. Valeev and A. Shevelev, "Design of WAG Parameters," *SPE Russian Petroleum Technology Conference*. Society of Petroleum Engineers, Moscow, Russia, p. 8, 2017, doi: 10.2118/187843-MS.

[26] G. of Canada, "Natural Resources Canada BASIN Database," 2021. https://basin.gdr.nrcan.gc.ca/wells/index_e.php (accessed Jan. 07, 2021).

[27] M. C. Leverett, "Capillary Behavior in Porous Solids," *Trans. AIME*, vol. 142, no. 01, pp. 152–169, 1941, doi: 10.2118/941152-G.

[28] B. Harrison and X. Jing, "Saturation Height Methods and Their Impact on Volumetric Hydrocarbon in Place Estimates," Sep. 2001, doi: 10.2118/71326-MS.

[29] F. Lomeland, E. Ebeltoft, and W. Thomas, *A New Versatile Relative Permeability Correlation*. 2005.

[30] L. S. School, "Typical schematic of polymer waterflooding process," *Low Shear School Webpage*, 2021. http://www.lowshearschool.com/?page_id=17110 (accessed Jan. 23, 2021).

Appendix A: UHQ Test Results with WAG Hysteresis

The chart within Appendix A contains the simulation case results for a test of the impact of the hysteresis functionality. The results displayed were used to evaluate the impact of implementing hysteresis in the dynamic model.

The test case used Killough's hysteresis model for the non-wetting phases and used the drainage curve from the wetting phase. For this test case, the Ultra-High-Quality sector model is simulated using WAG depletion with the light oil fluid model.

The results and impact of hysteresis are further discussed in Section 4.1.4.

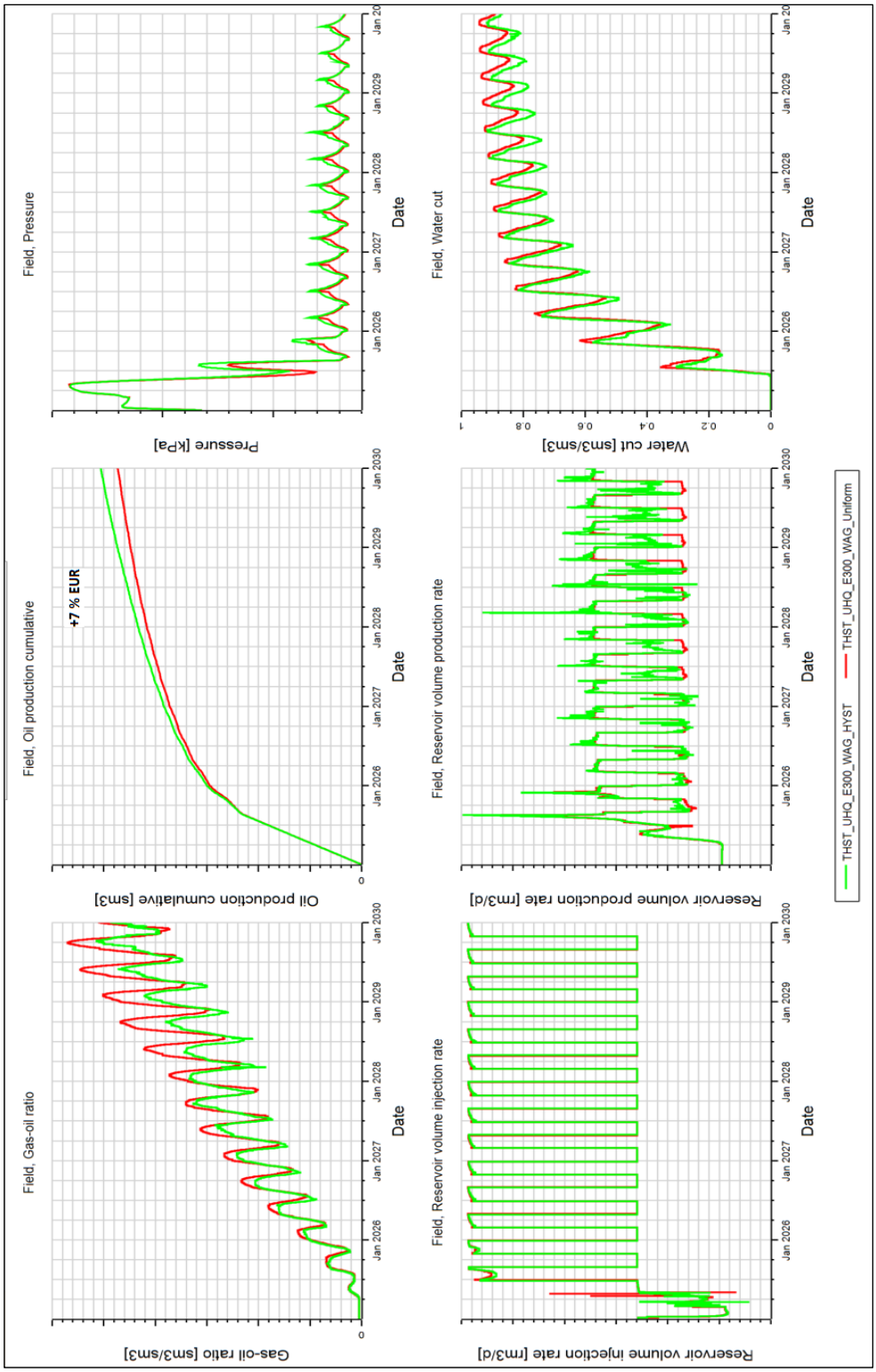

Figure 33: Simulation Results comparing UHQ Light Oil cases with and without WAG Hysteresis